Self-consistent mean-field approach to the statistical level density in spherical nuclei

V. M. Kolomietz, A. I. Sanzhur, and S. Shlomo

Phys. Rev. C **97**, 064302 — Published 4 June 2018

DOI: 10.1103/PhysRevC.97.064302

Self-consistent mean field approach to the statistical level density in spherical nuclei

V.M. Kolomietz,[1] A.I. Sanzhur,[1] and S. Shlomo[2,3]

[1] *Institute for Nuclear Research, 03680 Kiev, Ukraine*

[2] *Cyclotron Institute, Texas A&M University,*

College Station, Texas 77843, USA

[3] *Department of Elementary Particles and Astrophysics,*

the Weizmann Institute of Science, Rehovot 76100, Israel

Abstract

A self consistent mean-field approach within the extended Thomas-Fermi approximation with Skyrme forces is applied to the calculations of the statistical level density in spherical nuclei. Landau's concept of quasiparticles with the nucleon effective mass and the correct description of the continuum states for the finite-depth potentials are taken into consideration. The A-dependence and the temperature dependence of the statistical inverse level-density parameter K is obtained in a good agreement with experimental data.

PACS numbers: 21.65.+f, 24.10.Pa

I. INTRODUCTION

The methods of statistical physics and thermodynamics is an essential element of the theory of highly excited nuclei. Applications of statistical methods in nuclear physics cover many observable characteristics such as the statistical level density, the resonance energies and widths, the average cross-sections of nuclear reactions, the yields in nuclear fission, etc. The statistical level density $\varrho(E_{\rm ex})$ for a given excitation energy $E_{\rm ex}$ is the subject of many theoretical and experimental investigations in nuclear physics [1–8]. The excitation energy $E_{\rm ex}$ is referred to the ground state energy E_0 and reads $E_{\rm ex} \equiv E_{\rm ex}(T) = E(T) - E_0 = aT^2$, where T is the temperature, $E(T)$ is the total energy and a is the statistical level density parameter.

A key element in the study of the statistical level density $\varrho(E_{\rm ex})$ is the single-particle level density $g(\epsilon)$, associated with the nuclear mean field and the nuclear shell model of the non-interacting nucleons [2]. The basic fact is that in a low temperature limit, where temperature $T \ll \epsilon_F$ (ϵ_F is the Fermi energy), the excitation energy $E_{\rm ex}$ of a strongly interacting Fermi-system is determined mainly by the variation of the occupation number $\delta n(\epsilon)$ in close vicinity to the Fermi energy ϵ_F, see also Fig. 1 below. This fact allows us to apply the Landau's concept of Fermi-gas of quasi-particles [9, 10] to the strongly interacting nucleons. The excitation energy $E_{\rm ex}$ of a nucleus is then associated with the excitation of the gas of noninteracted quasi-particles.

The spin-independent part of the statistical level density $\varrho(E_{\rm ex}) \sim \exp S(E_{\rm ex})$ is related to the entropy $S(E_{\rm ex})$ and can be evaluated by use of the Darvin-Fowler method [1, 5, 6]

$$\varrho(E_{\rm ex}) = \frac{\sqrt{\pi}}{12\ a^{1/4}\ E_{\rm ex}^{5/4}} \exp\left(2\sqrt{aE_{\rm ex}}\right) = \frac{\sqrt{\pi}}{12\ a^{3/2}\ T^{5/2}} \exp\left(2aT\right). \tag{1}$$

The evaluation of the excitation energy $E_{\rm ex}(T)$ of a Fermi gas is shown in Appendix A. Using Eq. (A9) of Appendix A, one can obtain the commonly used expression for the statistical level density parameter a [2]

$$a = \frac{1}{6}\pi^2 g(\epsilon_F) + \mathcal{O}(T^2). \tag{2}$$

The simple Fermi-gas result (2) within the traditional shell-model consideration overestimates the inverse level density parameter $K = A/a$ by factor of about 2, see e.g. Ref. [8]. To improve an agreement of K with the experimental data, in many practical calculations

one took into consideration the effects of correlated interaction, pairing effects, rotation and vibration states, temperature dependence, etc. [2, 4, 6, 7, 11–30]. One can, however, expect that for the highly excited nuclei at the excitation energy $E_{\rm ex}$ of order of the nuclear separation energy $E_{\rm ex} \propto 7 \div 8$ MeV and higher, where the interlevel distance $\Delta E = 1 \div 10$ eV is much smaller than the effect of the strong interparticle (residual) interaction $v_{\rm int} \gg \Delta E$, the interparticle interaction does not perturb essentially the average level distribution and the statistical level density $\varrho(E_{\rm ex})$ and only leads to interlevel mixing. Moreover, multi-particle-hole excitations which are generated by a nuclear mean field give a *full set* of states and the residual interaction provides only a redistribution of these states. Thus, it can be expected that a reasonable results for the statistical level-density calculations can be obtained within the shell-model [8] by the condition of an appropriate evaluation of the single-particle level density $g(\epsilon)$. Note also that a correct use of a realistic finite depth potential well, such as Woods-Saxon (WS) or Hartree-Fock (HF) mean fields, for calculations of the statistical level density of highly excited nuclei requires the knowledge of the single-particle level density $g(\epsilon)$ for a wide range of ϵ, including the continuum region [8]. In particular, a proper accounting for the continuum states is also important for determining the temperature dependence of the statistical level density parameter a and the nuclear properties in the case of the preequilibrium decay from states with a small exciton number [31, 32]. The study of the temperature dependence of the statistical level density parameter, a, was stimulated by experimental data [33–35] for nuclei with $A \sim 160$, where the temperature dependence of a was deduced from coincidence measurements between heavy residues, light particles and γ -rays. In more recent publication [25, 28] for the temperature dependence of the statistical level density parameter was extracted for nuclei close to ^{208}Pb from neutron evaporation spectra and proton scattering.

The microscopic description of the statistical level density can be effectively performed within Hartree-Fock (HF) and Hartree-Fock-Bogolubov (HFB) approaches, see in particular Refs. [26, 27]. Note however that both the HF and the HFB approaches are well-defined for zero temperature only. Note also that the Darvin-Fowler method is not necessary ingredient in the calculations of the statistical level density. As it was noted in the pioneering work by Ericson [1] the combinatorial methods can be also used. Further progress in this direction was demonstrated in Refs. [23, 29].

In the present work we use the extended Thomas-Fermi (ETF) approximation with the

effective Skyrme nucleon-nucleon interaction to evaluate the nuclear mean field $V_{\rm ETF}(\mathbf{r})$ and the single-particle level density $g(\epsilon)$. Our aim is to study the possibility of description of the average statistical level density $\varrho(E_{\rm ex})$ within the semiclassical ETF. Note that in the framework of the used ETF approximation, the nuclear mean field $V_{\rm ETF}(\mathbf{r})$ is self-consistent. Namely, the mean field $V_{\rm ETF}(\mathbf{r})$ depends on the particle density $\rho(\mathbf{r})$ which is determined by the variational principle and based on the effective nucleon-nucleon interaction only. The ETF particle density $\rho(\mathbf{r})$ and thereby the mean field $V_{\rm ETF}(\mathbf{r})$ do not contain the quantum shell oscillations. This fact can be used for the practical applications of the ETF mean field $V_{\rm ETF}(\mathbf{r})$ for calculations of the nuclear mass and the deformation energy within the Strutinsky's shell correction method. The basic elements of the shell correction method are the liquid drop model (LDM) and the shell-model mean field $V(\mathbf{r})$. The commonly used Woods-Saxon potential $V_{\rm WS}(\mathbf{r})$ (instead of $V(\mathbf{r})$) is a phenomenological one and it is not consistent with the basic LDM. This defect can not be overcome by use, for example, the selfconsistent Hartree-Fock mean field $V_{\rm HF}(\mathbf{r})$. The Hartree-Fock mean field $V_{\rm HF}(\mathbf{r})$ includes the quantum shell oscillations and thereby can not be consistent with averaged characteristics of the LDM.

Note that the ETF is a semiclassical approach and it can not be directly used to describe the shell structure of the level density parameter a, in particular, the strong departure of the level density parameter a from a smooth behavior for nuclei in the vicinity of closed shells. This phenomenon was studied in detail near the nucleus ^{208}Pb in Ref. [28], where the back-shifted Fermi gas model was used to extract the level density parameter a from the statistical level density.

An advantage of our ETF approach is that it provides description for the liquid drop properties, including nuclear mass, deformation energy, fission barrier etc., see Refs, [36–39], the nuclear mean field $V_{\rm ETF}(r)$ and correspondingly the smooth behavior of the statistical level density. This fact allows one to evaluate the quantum shell corrections consistently with the liquid-drop mass formula within Strutinsky shell-correction method avoiding the introducing of the phenomelogical shell-model mean field. Our results can be also considered as a test of the ability of the ETF approach to describe the smooth statistical properties of hot nuclei. Moreover we represent a detailed analysis of the influence of the effective nucleon masses and the single particle state in continuum on the statistical level density parameter in hot nuclei.

Note that a good description of the statistical level density in a wide interval of mass number requires to take into consideration the quantum shell effects, the pairing correlations and the nuclear deformation. All these aspects can be studied by applying the Landau's conception of quasiparticles [40], which are localized near the Fermi surface, used in our approach. In particular, the effect of pairing correlations can be reduced to the quasiparticle description by employing the Bogolubov-Valatin transformation.

In Section II, we present the thermodynamic derivation of the statistical level density. The evaluation of the single particle level density within Thomas-Fermi (TF) and extended Thomas-Fermi (ETF) approximations is discussed in Section III. The numerical results for the nuclear excitation energy and the statistical level density parameter are given in Sections IV and V. The discussion of results and the conclusion are presented in Section VI.

II. STATISTICAL LEVEL DENSITY AND LANDAU'S CONCEPTION OF QUASIPARTICLES.

Considering the heated nuclei and the corresponding definition (1) of the statistical level density $\varrho(E_{\rm ex})$, one assumes high enough excitation energy $E_{\rm ex}$ such that the temperature T can be introduced in a small finite Fermi-system. In the low temperature limit $T \ll \epsilon_F$, the excitation energy $E_{\rm ex}(T)$ is given by the calorimetric relation $E_{\rm ex}(T) = aT^2$ which can be used for a simple thermodynamic derivation of the level density parameter

$$a = E_{\rm ex}(T)/T^2. \tag{3}$$

As mentioned above, evaluating the excitation energy $E_{\rm ex}$ of strongly interacting Fermi-system one can apply the Landau's conception of Fermi-gas of quasiparticles. This conception includes, in particular, the presence of the effective mass of nucleon m_q^* ($q = n$ for neutron and $q = p$ for proton) [10]. The excitation energy $E_{\rm ex}$ of Fermi-gas of nucleons of sort q is written as

$$E_{{\rm ex},q}(T) = E_q(T) - E_q(T=0) = \int d\epsilon\ \epsilon\ g_q(\epsilon)\ \delta n_q(\epsilon, T), \tag{4}$$

where $\delta n_q(\epsilon, T) = n_q(\epsilon, T) - \Theta(\epsilon_{F,q} - \epsilon)$, see Appendix A. The effective mass m_q^* enters into the derivation of the nuclear one-body Hamiltonian and thereby the single-particle level density $g_q(\epsilon)$.

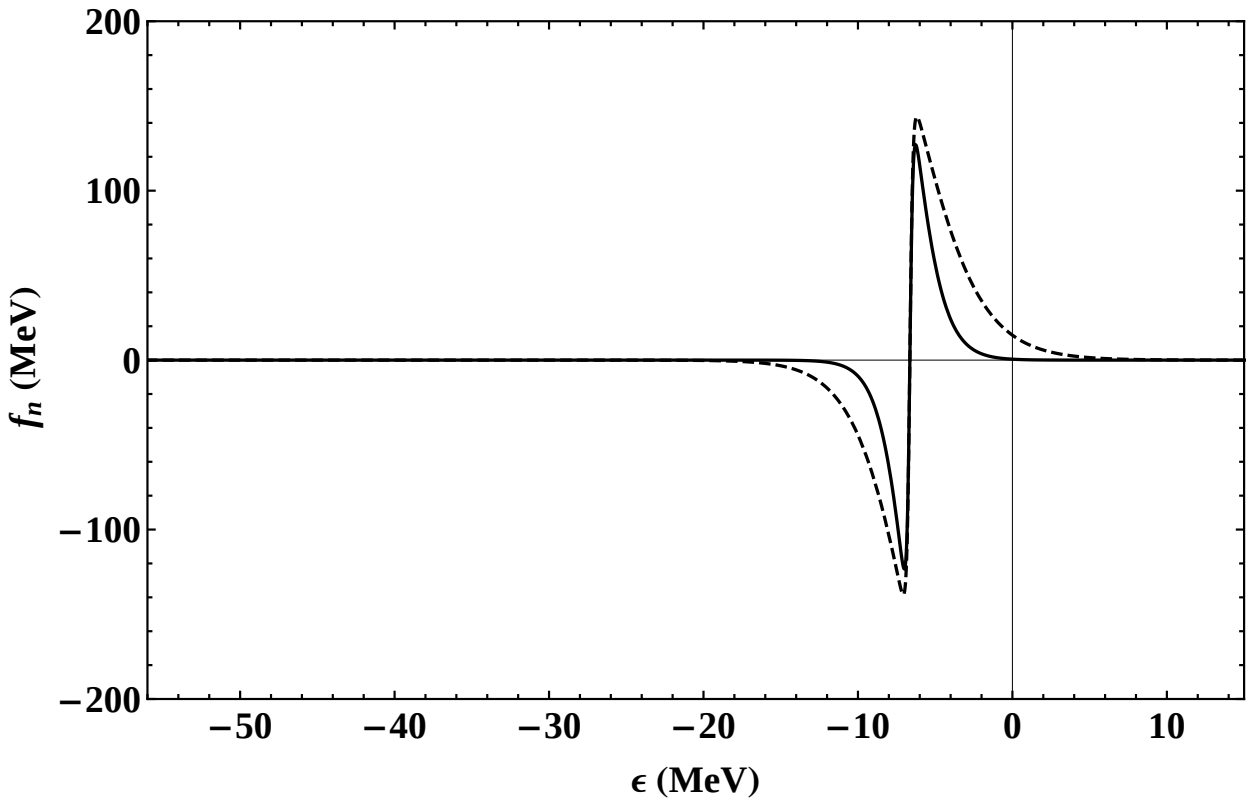

FIG. 1. The integrand $f_n(\epsilon) = \epsilon\ g_n(\epsilon)\ \delta n(\epsilon, T)$ in Eq. (4) for the neutron excitation energy $E_{\rm ex}$ for the nucleus ^{208}Pb. Solid line for $T = 1$ MeV and dashed line for $T = 5$ MeV. The single-particle level density $g_n(\epsilon)$ was calculated using Eqs. (7) and (27) and the mean field $V_n(r)$ from Fig. 4.

The Landau's concept of quasiparticles requires that the integrand $f(\epsilon) = \epsilon\ g(\epsilon)\ \delta n(\epsilon, T)$ in Eq. (4) should be localized near the Fermi energy ϵ_F. In Fig. 1 we have plotted the integrand $f(\epsilon)$ for the nucleus ^{208}Pb for two temperatures $T = 1$ MeV and $T = 2$ MeV.

As can be seen from Fig. 1, the integrand $f(\epsilon)$ of Eq. (4) is localized near the Fermi energy $\epsilon_{F,n}$ ($\epsilon_{F,n} \approx -\ 8$ MeV in Fig. 1) quite well. This fact confirms the Landau's conception of quasiparticles and allows one to use Eq. (4) to evaluate the excitation energy of a nucleus. Note also that for higher temperatures the integrand $f(\epsilon)$ in Eq. (4) penetrates into the region of continuum states $\epsilon > 0$ and the continuum effect on the single-particle level density (see also Sect. V) has to be taken into account (see dashed line in Fig. 1). Note that the excitation energy $E_{{\rm ex},q}$ as well as Fermi energy $\epsilon_{F,q}(T)$ are different for both the neutron and proton components. The expression (4) contains the single-particle level density $g_q(\epsilon)$ which is energy-dependent and the final result for a, in the case of finite depth potentials, can be

sensitive to the single-particle level distribution near the Fermi surface.

III. SINGLE PARTICLE LEVEL DENSITY WITHIN THE EXTENDED THOMAS-FERMI APPROXIMATION WITH SKYRME INTERACTION

Let us consider the number of particles $N(\epsilon)$ embedded in a potential well $V(\mathbf{r})$ with energy below ϵ. Using the Wigner distribution function in phase space $f(\mathbf{r},\mathbf{p})$, one can write

$$N(\epsilon) = 2\int \frac{d\mathbf{r}\; d\mathbf{p}}{(2\pi\hbar)^3}\; f(\mathbf{r},\mathbf{p})|_{p\le p_\epsilon}\,, \tag{5}$$

where the factor 2 in front of integral is due to the spin degeneracy and $p_\epsilon \equiv p_\epsilon(\mathbf{r})$ is derived by the following relation

$$\frac{p_\epsilon^2}{2m} \equiv \frac{p_\epsilon^2(\mathbf{r})}{2m} = \epsilon - V(\mathbf{r}). \tag{6}$$

Note that the expression (5) must be written for both the neutrons and the protons. The single-particle level density $g(\epsilon)$ is obtained from $N(\epsilon)$ by

$$g(\epsilon) = \frac{d}{d\epsilon}N(\epsilon). \tag{7}$$

A. *Thomas-Fermi approximation*

In the case of the Thomas-Fermi (TF) approximation, the distribution function $f_{\rm TF}(\mathbf{r},\mathbf{p})|_{p\le p_\epsilon}$ is given by a simple expression

$$f_{\rm TF}(\mathbf{r},\mathbf{p})|_{p\le p_\epsilon} = \Theta\left[\frac{p_\epsilon^2}{2m} - \left(\frac{p^2}{2m} + V(\mathbf{r})\right)\right]$$

and the number of particles $N(\epsilon)$ takes the form

$$N_{\rm TF}(\epsilon) = 2\int \frac{d\mathbf{r}\; d\mathbf{p}}{(2\pi\hbar)^3}\Theta\left[\frac{p_\epsilon^2}{2m} - \left(\frac{p^2}{2m} + V(\mathbf{r})\right)\right]. \tag{8}$$

Integrating in Eq. (8) over $\mathbf{p}$, one obtains

$$N_{\rm TF}(\epsilon) = \frac{1}{3\pi^2}\left(\frac{2m}{\hbar^2}\right)^{3/2}\int d\mathbf{r}[\epsilon - V(\mathbf{r})]^{3/2}\Theta\left[\epsilon - V(\mathbf{r})\right] \tag{9}$$

and the corresponding single-particle level density

$$g_{\rm TF}(\epsilon) = \frac{1}{2\pi^2}\left(\frac{2m}{\hbar^2}\right)^{3/2}\int d\mathbf{r}\ [\epsilon - V(\mathbf{r})]^{1/2}\Theta\left[\epsilon - V(\mathbf{r})\right] \tag{10}$$

The value of $N_{\rm TF}(\epsilon)$ taken at $\epsilon = \epsilon_F$ gives the total number of particles A in a Fermi system.

Note that the expression (9) can be written in the form which avoids the problem of the turning point at $\epsilon_F - V(\mathbf{r}) = 0$. Generalizing the extended Thomas-Fermi (ETF) approach [38, 39, 41], we will introduce the particle density $\rho_\epsilon(\mathbf{r})$ which corresponds to the number of particles $N(\epsilon)$ with energy $\epsilon \leq \epsilon_F$. The particle density $\rho_\epsilon(\mathbf{r})$ is derived by the following relation

$$N_{\rm TF}(\epsilon) = 2\int \frac{d\mathbf{r}\ d\mathbf{p}}{(2\pi\hbar)^3}\ f_{\rm TF}(\mathbf{r},\mathbf{p})\big|_{p\ \leq\ p_\epsilon} = \int d\mathbf{r}\ \rho_\epsilon(\mathbf{r}), \tag{11}$$

where we have used

$$p_\epsilon(\mathbf{r}) = \sqrt{2m[\epsilon - V(\mathbf{r})]}\Big|_{V(\mathbf{r})\ \leq\ \epsilon} = (3\pi^2\hbar^3)\rho_\epsilon^{1/3}(\mathbf{r}). \tag{12}$$

Accordingly, in the ETF approximation, the particle density $\rho_\epsilon(\mathbf{r})$ can be evaluated independently on Eq. (12) from the relevant variational procedure, see Appendix C.

B. *Extended Thomas-Fermi approximation*

The Thomas-Fermi approximation is extended taking into consideration the corrections up to order of $\hbar^2$ in the Kirkwood $\hbar$-expansion of distribution function $f(\mathbf{r},\mathbf{p})$. The corresponding extended Thomas-Fermi distribution function $f_{\rm ETF}(\mathbf{r},\mathbf{p})$ reads [42, 43]

$$\begin{aligned} f_{\rm ETF}(\mathbf{r},\mathbf{p})\big|_{p\leq p_\epsilon} = \Theta\left[\frac{p_\epsilon^2}{2m} - \frac{p^2}{2m}\right] + \frac{\hbar^2}{8\,m}\ \Big\{(\nabla^2 V)\,\frac{d}{dE}\delta(E) \\ + \frac{1}{3}\left[(\nabla V)^2 + \frac{1}{m}\,(\mathbf{p}\cdot\nabla)^2 V\right]\frac{d^2}{dE^2}\delta(E)\Big\} \end{aligned} \tag{13}$$

where $E = p^2/2m - p_\epsilon^2/2m = p^2/2m - [\epsilon - V(\mathbf{r})]$. Substituting Eq. (13) into Eq. (5) and integrating over $\mathbf{p}$, we obtain

$$N_{\rm ETF}(\epsilon) = 2\int \frac{d\mathbf{r}\ d\mathbf{p}}{(2\pi\hbar)^3}\ f_{\rm ETF}(\mathbf{r},\mathbf{p})\big|_{p\leq p_\epsilon} \tag{14}$$

$$= N_{\rm TF}(\epsilon) - \frac{1}{24\pi^2}\sqrt{\frac{2m}{\hbar^2}}\int d\mathbf{r}\left[\frac{\nabla^2 V(\mathbf{r})}{[\epsilon - V(\mathbf{r})]^{1/2}} + \frac{1}{4}\frac{[\nabla V(\mathbf{r})]^{\,2}}{[\epsilon - V(\mathbf{r})]^{3/2}}\right]\Theta\left[\epsilon - V(\mathbf{r})\right] \tag{15}$$

Applying the identity

$$\frac{(\nabla V)^2}{[\epsilon - V]^{3/2}} = 2\nabla \cdot \frac{\nabla V}{[\epsilon - V]^{1/2}} - 2\frac{\nabla^2 V}{[\epsilon - V]^{1/2}}$$

we will rewrite Eq. (15) as

$$N_{\rm ETF}(\epsilon) = N_{\rm TF}(\epsilon) - \frac{1}{48\ \pi^2}\sqrt{\frac{2m}{\hbar^2}} \int d\mathbf{r} \left[\frac{\nabla^2 V(\mathbf{r})}{[\epsilon - V(\mathbf{r})]^{1/2}} + \nabla \cdot \frac{\nabla V}{[\epsilon - V]^{1/2}} \right] \Theta\left[\epsilon - V(\mathbf{r})\right]. \quad (16)$$

Using the relation (12), the turning point can be eliminated from the consideration and Eq. (16) takes the following form

$$N_{\rm ETF}(\epsilon) = N_{\rm TF}(\epsilon) - \frac{1}{48\ \pi^2}\frac{2m}{\hbar^2}\frac{1}{(3\pi^2)^{1/3}} \int d\mathbf{r}\ \left[\rho_\epsilon^{-1/3}(\mathbf{r})\ \nabla^2 V(\mathbf{r}) + \nabla \cdot \rho_\epsilon^{-1/3}(\mathbf{r})\ \nabla V\right]. \quad (17)$$

Using then the Gauss-Ostrogradsky theorem [44] and the fact that asymptotically on the outlying surface $V(\mathbf{r}) \sim \rho(\mathbf{r})$, we reduce Eq. (17) to the following form

$$N_{\rm ETF}(\epsilon) = N_{\rm TF}(\epsilon) - \frac{1}{48\ \pi^2}\frac{2m}{\hbar^2}\frac{1}{(3\pi^2)^{1/3}} \int d\mathbf{r}\ \rho_\epsilon^{-1/3}(\mathbf{r})\ \nabla^2 V(\mathbf{r}), \quad (18)$$

where $N_{\rm TF}(\epsilon)$ is given by Eq. (11).

C. *Selfconsistent mean field $V(\mathbf{r})$ within the ETF approximation*

The selfconsistent mean field $V(r)$ can be derived within the variational procedures of ETF approximation. The total energy E of the nucleus within the ETF approximation is given by

$$E = E_{\rm kin} + E_{\rm pot} \quad (19)$$

where

$$E_{\rm kin} = \int d\mathbf{r}\ \epsilon_{\rm kin}[\rho_n(\mathbf{r}), \rho_p(\mathbf{r})], \quad E_{\rm pot} = \int d\mathbf{r}\ \epsilon_{\rm pot}[\rho_n(\mathbf{r}), \rho_p(\mathbf{r})]. \quad (20)$$

Here, the kinetic energy density $\epsilon_{\rm kin}$ and the potential energy density $\epsilon_{\rm pot}$ depend on the particle density ρ_q ($q = n$ for neutron and $q = p$ for proton) and its gradient only. The

standard ETF variational procedure implies that the unknown values of ρ_n and ρ_p can be evaluated from the variational principle

$$\delta(E - \lambda_n N - \lambda_p Z) = 0, \tag{21}$$

where the variation with respect to all possible small changes of ρ_n and ρ_p is assumed. The Lagrange multipliers λ_n and λ_p in Eq. (21) are derived from the condition of conservation for the numbers of neutrons N and protons Z. The potential energy density $\epsilon_{\rm pot}[\rho_n(\mathbf{r}), \rho_p(\mathbf{r})]$ of the nucleon-nucleon interaction, includes the effective nucleon-nucleon interaction (we will use Skyrme forces $\epsilon_{\rm Sk}[\rho_n, \rho_p]$) and the Coulomb energy density, $\epsilon_{\rm C}[\rho_p]$,

$$\epsilon_{\rm pot}[\rho_n, \rho_p] = \epsilon_{\rm Sk}[\rho_n, \rho_p] + \epsilon_{\rm C}[\rho_p]\delta_{qp}. \tag{22}$$

Within the framework of ETF approximation, the kinetic energy density $\epsilon_{\rm kin}[\rho_n, \rho_p]$ includes also the density-gradient terms [42, 43].

To evaluate the nucleon density ρ_q and solve the variational equation (21), we will apply the direct variational method using a trial function for $\rho_q(\mathbf{r})$ in the following form, see Refs. [36, 38],

$$\rho_q(\mathbf{r}) = \rho_{0,q}\left[1 + \exp\left(\frac{r - R_q}{d_q}\right)\right]^{-\eta_q}, \tag{23}$$

where $\rho_{0,q}$, R_q, d_q and η_q are the unknown variational parameters which are obtained by solving Eq. (21). In Table I we show the evaluated variational parameters $\rho_{0,q}$, R_q, d_q and η_q for several spherical nuclei.

Note that the obtained particle density $\rho_q(\mathbf{r})$ of Eq. (23) and Table I provides the bulk, surface and symmetry energies in a good agreement with the experimental data given by the Weizsäcker mass formula, see Ref. [36].

The nuclear mean field $V_q(\mathbf{r})$ is obtained as a functional derivative of potential energy $E_{\rm pot}$.

$$V_q(\mathbf{r}) = \frac{\delta}{\delta\rho_q}E_{\rm pot} = \left[\frac{\partial}{\partial\rho_q} - \nabla\frac{\partial}{\partial(\nabla\rho_q)} + \nabla^2\frac{\partial}{\partial(\nabla^2\rho_q)}\right]\epsilon_{\rm pot}[\rho_n, \rho_p], \tag{24}$$

where $\epsilon_{\rm pot}[\rho_n, \rho_p]$ is the potential energy density. An explicit form of the nuclear mean field $V_q(\mathbf{r})$ for the Skyrme interaction is presented in Appendix B. In Fig. 2 we show the result for $V_q(\mathbf{r})$ from Eq. (B1) of Appendix B for the nucleus ^{208}Pb for the SkM* interaction with the nucleon density $\rho_q(\mathbf{r})$ from Eq. (23) and Table I. The obtained selfconsistent mean field is quite similar to the standard Woods-Saxon potential with a smaller surface region of the potential wall.

TABLE I. Particle density parameters $\rho_{0,q}$, R_q, d_q(in fm) and η_q for spherical nuclei ^{40}Ca, ^{48}Ca, ^{90}Zr, ^{120}Sn and ^{208}Pb obtained from the variational principle of Eq. (21) for the SkM* [39] and KDE0v1 [45] interactions.

	SkM*					KDE0v1				
	^{40}Ca	^{48}Ca	^{90}Zr	^{120}Sn	^{208}Pb	^{40}Ca	^{48}Ca	^{90}Zr	^{120}Sn	^{208}Pb
$\rho_{0,n}$	0.0874	0.0955	0.0903	0.0920	0.0914	0.0893	0.0974	0.0923	0.0940	0.0934
$\rho_{0,p}$	0.0837	0.0743	0.0734	0.0684	0.0620	0.0859	0.0760	0.0754	0.0703	0.0637
R_n	5.5463	5.4760	6.6080	7.0189	8.0999	5.3333	5.2422	6.3749	6.7776	7.8455
R_p	5.3134	5.7384	6.5235	7.0135	8.0181	5.1453	5.5944	6.3831	6.8873	7.9085
d_n	0.7220	0.7542	0.7379	0.7350	0.7234	0.7074	0.7059	0.6943	0.6894	0.6766
d_p	0.7484	0.7109	0.6780	0.6602	0.6177	0.6837	0.6788	0.6470	0.6323	0.5944
η_n	8.4990	5.1159	6.0887	4.9526	4.0474	7.4716	4.3567	5.2556	4.2314	3.4208
η_p	6.3130	9.0405	6.5326	6.4561	5.1581	5.7986	8.5417	6.2350	6.2634	5.1160

D. *Continuum effect on the single-particle level density*

For a finite depth potential $V(r)$ the single-particle level density $g(\epsilon)$ includes both the bound-state and the continuum-state contributions. The numerical calculations of the level density $g(\epsilon)$ requires a high accuracy to prevent a spurious contribution to the excitation energy $E_{\rm ex}$ given by Eq. (4). Such kind of spurious contribution occurs due to the free space states which are not associated with the finite potential well $V(r)$. The corresponding (spurious) free-space number of states $N_{\rm free}(\epsilon)$ is obtained by integrating over the free-space states $2d\mathbf{r}d\mathbf{p}/(2\pi\hbar)^3$ and it is given by [8]

$$N_{\rm free}(\epsilon) = \frac{1}{3\pi^2}\left(\frac{2m}{\hbar^2}\right)^{3/2}\int d\mathbf{r}\ \epsilon^{3/2}\ \Theta(\epsilon) \tag{25}$$

The number of states of Eq. (18) should be corrected by subtracting the contribution $N_{\rm free}(\epsilon)$. Below, we will restrict ourselves to a spherical mean field $V(r)$. The final result for the number of states reads

$$\widetilde{N}_{\rm ETF}(\epsilon) = \widetilde{N}_{\rm TF}(\epsilon) - \frac{1}{12\pi}\int_0^\infty dr\ \left(\frac{2m}{\hbar^2}\right)^{1/2} r^2 \frac{\Theta\left[\epsilon - V(r)\right]}{\left[\epsilon - V(r)\right]^{1/2}}\left[\frac{\partial^2}{\partial r^2}V(r) + \frac{2}{r}\frac{\partial}{\partial r}V(r)\right], \tag{26}$$

where

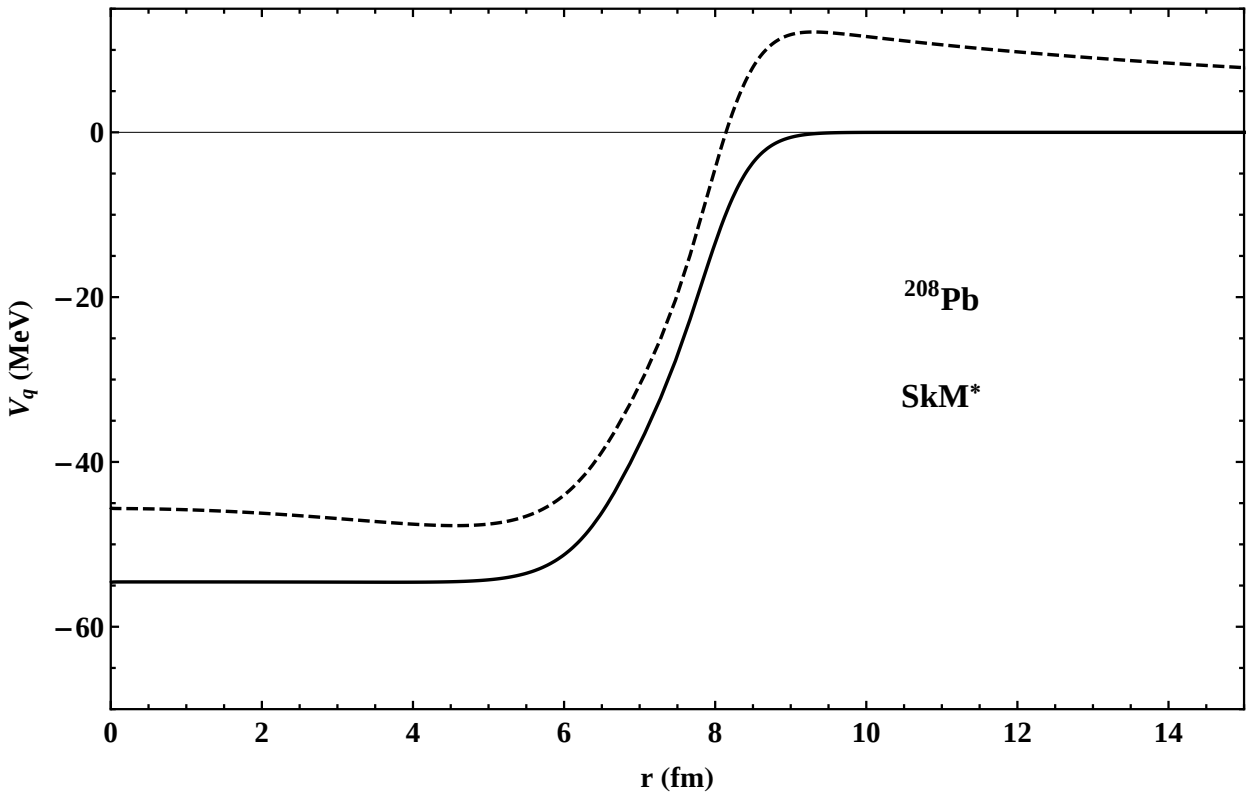

FIG. 2. The self-consistent mean field $V_q(r)$ given by Eq. (B1) (see Appendix B) with the ETF particle density $\rho_q(r)$ from Eq. (23) and Table 1 for the nucleus ^{208}Pb for the SkM* interaction [39]. The solid line is the neutron mean field $V_n(r)$ and the dashed line is for the proton one $V_p(r)$.

$$\widetilde{N}_{\rm TF}(\epsilon) = \frac{4}{3\pi}\int dr \left(\frac{2m}{\hbar^2}\right)^{3/2} \; r^2 \; \left\{[\epsilon - V(r)]^{3/2}\Theta\left[\epsilon - V(r)\right] - \epsilon^{3/2}\;\Theta(\epsilon)\right\}. \qquad (27)$$

Note that the procedure of subtracting of the free-space state contribution $N_{\rm free}(\epsilon)$ from the continuum states agrees with the results of phase-shift approach and Green's function approach to the calculations of the single-particle levels (resonance states) in continuum, see Refs. [8, 21, 46, 47]. In particular, the subtraction of the free-space state contribution $N_{\rm free}(\epsilon)$ fulfils the Levinson's theorem [48] which establishes the relation between the phase shift at zero energy and the number of bound states.

E. *Effective mass*

As already mentioned above, we use the Landau's conception of the quasiparticles to derive the excitation energy $E_{\rm ex}(T)$ and thereby the level density parameter a, see Eqs. (3) and (4). The quasiparticle conception implies that the effective mass m^* of quasiparticle appears in the one-body Hamiltonian $h^* = p^2/2m^* + V$ and the mass m in Eqs. (15) and (18) must be replaced by the effective mass m^*. Note that the nucleon effective mass is, in general, r-dependent $m^* \equiv m^*(r)$ and can include contributions caused by the non-locality of the nucleon-nucleus interaction [49] (momentum dependent k-mass $m^*_k(r)$) and the long-range correlation corrections which arise, in particular, because of the scattering of nucleons from low-lying surface vibrations of the nucleus [50] (frequency dependent ω-mass $m^*_\omega(r)$), see also Refs. [8, 12, 13].

In the case of local shell-model potentials, such as Woods-Saxon, one of the consequence of such kind of replacement $m \to m^*$ is that the Fermi energy ϵ_F is shifted up. This effect can be easily seen for the infinite square-well potential $V_{\rm SQ}$. In this case, the bulk Fermi-momentum $p_{F,0} \sim \rho_0^{1/3}$ is r-independent. The nuclear bulk density ρ_0 does not depend on m. Therefore, a shift up of the Fermi energy $\epsilon_{F,0} = p^2_{F,0}/2m \to \epsilon^*_{F,0} = p^2_{F,0}/2m^* > p^2_{F,0}/2m$ violates the mentioned consistency of the bulk Fermi-momentum and the bulk density. To prevent such kind of violation one needs the corresponding shift of the mean field $V_{\rm SQ}$ in the one-body Hamiltonian $h^*_{\rm SQ}$ using a relevant modification of the mean field $V_{\rm SQ}$, see also Ref. [8],

$$V_{\rm SQ} \to V^*_{\rm SQ} = \frac{m}{m^*} V_{\rm SQ}.$$

A similar modification can be also applied to the phenomenological shell-model potential such as Woods-Saxon $V_{\rm WS}(r)$. Namely,

$$V_{\rm WS}(r) \to V^*_{\rm WS}(r) = \frac{m}{m^*(r)} V_{\rm WS}(r). \tag{28}$$

The expressions (26) and (27) have to be modified accordingly with replacing $V(r)$ by $V^*(r)$.

For the case of the Skyrme interaction, the self-consistent mean field $V_q(r)$ given by Eqs. (B1), (B2) and (B7) of Appendix B includes the modification due to the momentum-dependent effective k-mass $m^*_{q,k}(r) = m/f_q(r)$, where $f_q(r)$ is derived in Eq. (B4). However the modification caused by the correlation corrections to the effective mass (frequency-

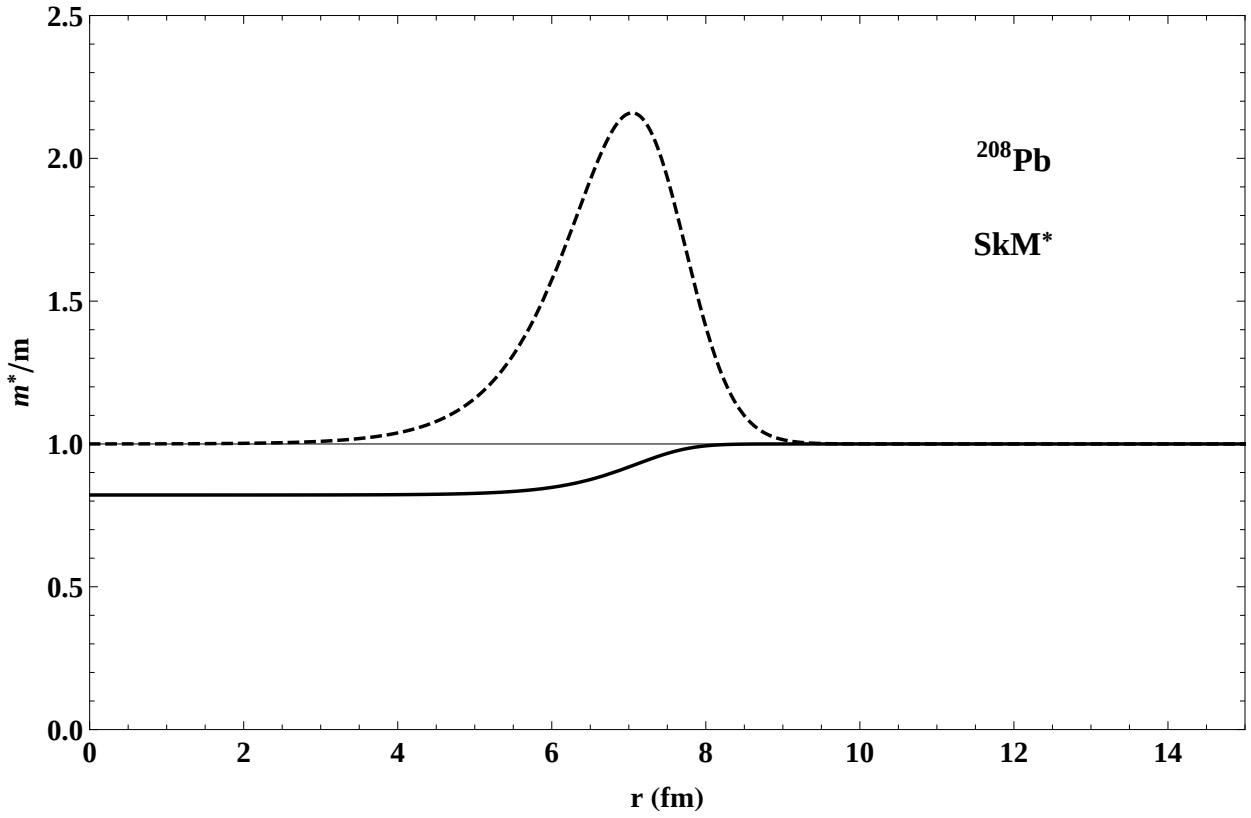

FIG. 3. The r-dependence of the momentum-dependent effective mass $m^*_{n,k}(r)/m$ generated by the Skyrme interaction (solid line) and the frequency dependent effective mass $m^*_{n,\omega}(r)/m$ (dashed line) for neutrons in the nucleus ^{208}Pb for SkM* interaction [39].

dependent effective ω-mass $m^*_{q,\omega}(r)$) must be added in this case. The effective mass $m^*_q(r)$ and the modified mean field $V^*_q(r)$ are then given by

$$m^*_q(r) = m^*_{q,k}(r)\ \frac{m^*_{q,\omega}(r)}{m} = \frac{m^*_{q,\omega}(r)}{f_q(r)}, \quad V^*_q(r) = \frac{m}{m^*_{q,\omega}(r)} V_q(r). \tag{29}$$

For the effective ω-mass $m^*_{q,\omega}(r)$ we will use the following form [12, 13],

$$\frac{m^*_{q,\omega}(r)}{m} = 1 - \beta \frac{d}{dr}\frac{\rho_q(r)}{\rho_{0,q}}, \tag{30}$$

where $\beta = 0.4\ A^{1/3}$ fm. The numerical results for the momentum-dependent k-mass $m^*_k(r)$ and the frequency dependent ω-mass $m^*_{q,\omega}(r)$ for neutrons in the nucleus ^{208}Pb obtained with SkM* interaction are shown in Fig. 3.

The presence of the frequency dependent ω-mass $m^*_{q,\omega}(r)$ reduces strongly the effective mean field $V^*_q(r)$ in the nuclear interior. The corresponding result for the nucleus ^{208}Pb is shown in Fig. 4.

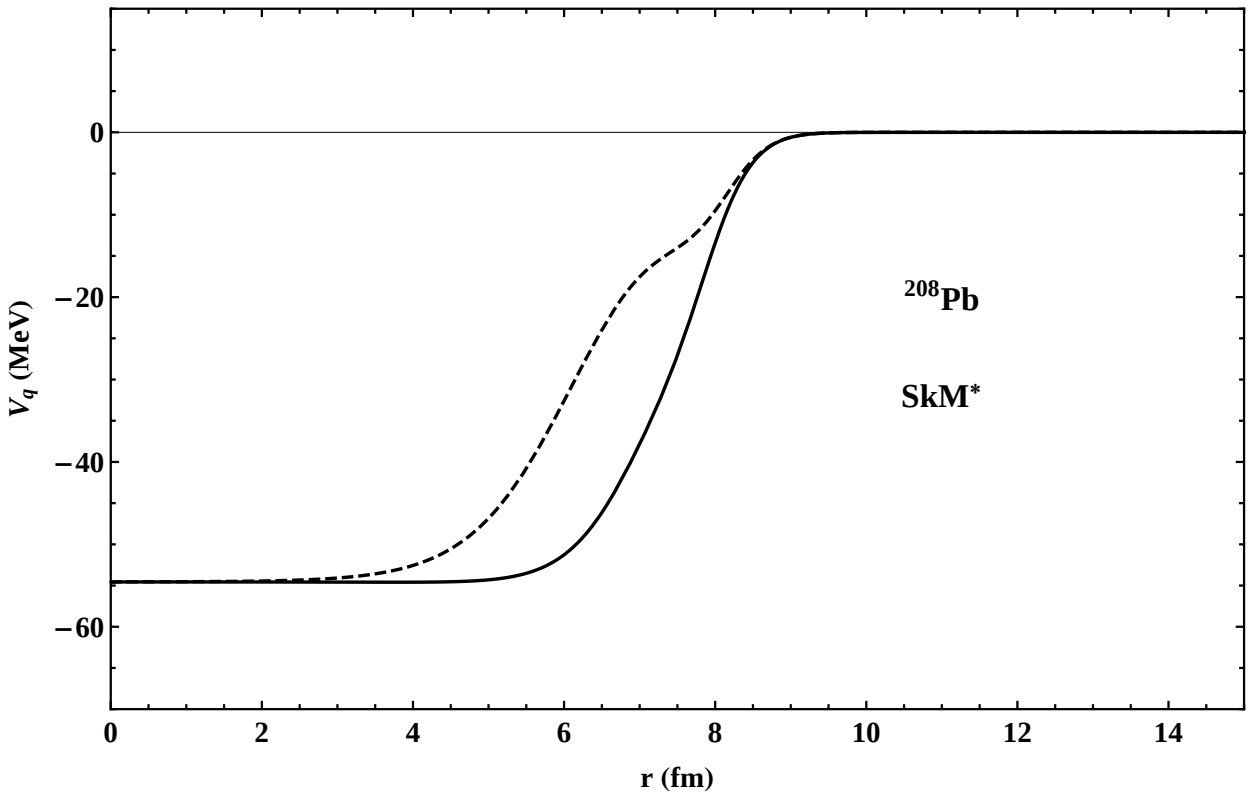

FIG. 4. The neutron SkM* mean field $V_n(r)$ (solid line) and the corresponding reduced mean field $V_n^*(r)$ from Eq. (29) (dashed line) in the nucleus ^{208}Pb.

Due to the distortion of the mean field $V_n^*(r)$ in the nuclear interior in Fig. 4, the Fermi energy $\epsilon_{F,n}$ is shifted up and the single particle levels are condensed in vicinity of $\epsilon_{F,n}$ increasing thereby both the particle level density $g(\epsilon_F)$ and the statistical level density parameter a, see Eq. (2).

Taking into account Eqs. (26), (27) and (29), the final result for the number of states $N_q(\epsilon)$ in the case of Skyrme interaction is given by

$$\widetilde{N}^*_{\mathrm{ETF},q}(\epsilon) = \widetilde{N}^*_{\mathrm{TF},q}(\epsilon) - \frac{1}{12\pi}\int_0^\infty dr\; r^2 \left(\frac{2m_q^*(r)}{\hbar^2}\right)^{1/2} \frac{\Theta\left[\epsilon - V_q^*(r)\right]}{\left[\epsilon - V_q^*(r)\right]^{1/2}} \left[\frac{\partial^2 V_q^*(r)}{\partial r^2} + \frac{2}{r}\frac{\partial V_q^*(r)}{\partial r}\right] \tag{31}$$

where

$$\widetilde{N}^*_{\mathrm{TF},q}(\epsilon) = \frac{4}{3\pi}\int dr \left(\frac{2m_q^*(r)}{\hbar^2}\right)^{3/2} r^2 \;\left\{\left[\epsilon - V_q^*(r)\right]^{3/2}\Theta\left[\epsilon - V_q^*(r)\right] - \epsilon^{3/2}\;\Theta(\epsilon)\right\}. \tag{32}$$

Using Eqs. (7) and (32), one can write the final TF expression for the single particle level

density as

$$\widetilde{g}^*_{\mathrm{TF},q}(\epsilon) = \frac{2}{\pi}\int dr \left(\frac{2m^*_q(r)}{\hbar^2}\right)^{3/2} r^2 \ \left\{[\epsilon - V^*_q(r)]^{1/2}\Theta\left[\epsilon - V^*_q(r)\right] - \epsilon^{1/2}\ \Theta(\epsilon)\right\}. \qquad (33)$$

F. *Single particle level density*

Evaluating the single particle level density $g(\epsilon)$, we will apply the ETF selfconsistent potentials $V_q(r)$ and $V^*_q(r)$ derived in Eqs. (B1) and (29), see also Fig. 4**.** In Fig. 5 we show the neutron single-particle level density for the nucleus^{208}Pb obtained with Skyrme interaction SkM*[39] by using Eq. (33). The dashed lines are obtained without subtraction of the free gas states.

As one can see from Fig. 5, the subtraction of the free gas states reduces significantly the single-particle level density for $\epsilon > 0$. Note also that, due to the finite size of the nuclear potential well, one has for the continuum region $\epsilon > 0$ that $g(\epsilon)$ decreases with increasing ϵ. That means that a proper treatment of the continuum is important for determining nuclear properties such as the level density of hot nuclei and the particle-hole level densities at high excitation energy. The result of Fig. 5 shows also a significant change of the behavior of level density $g(\epsilon)$ near the Fermi-energy ($\epsilon_{F,n} \approx -$ 8 MeV) in presence of the ω-mass $m^*_{q,\omega}$. The presence of effective ω-mass leads to the condense of the single particle levels near the Fermi surface because of the above mentioned features of the modified potential $V^*_n(r)$ (see Fig. 4) and thereby enhances the level density $g(\epsilon)$ near the edge of the potential well. We point out also that the density of free gas states (dashed lines in Fig. 5) depends on the choice of the radius R_{ext} of an external box. In numerical calculations in Fig. 5 and below we have used $R_{\mathrm{ext}} = 10$ fm.

The $\hbar^2$-corrections and the corresponding ETF values of the level density $g(\epsilon)$ and the number of particles $N(\epsilon)$ can be evaluated using Eqs. (7) and (26). For the $\hbar^2$-correction $N_{q,\mathrm{corr}}(\epsilon)$ to the number of particles one obtains (see Eqs. (26) and (27))

$$N_{\mathrm{corr}}(\epsilon) = -\frac{1}{12\pi}\int_0^\infty dr\ \left(\frac{2m^*_q}{\hbar^2}\right)^{1/2} r^2 \frac{\Theta\left[\epsilon - V^*_q(r)\right]}{\left[\epsilon - V^*_q(r)\right]^{1/2}}\left[\frac{\partial^2}{\partial r^2}V^*_q(r) + \frac{2}{r}\frac{\partial}{\partial r}V^*_q(r)\right]. \qquad (34)$$

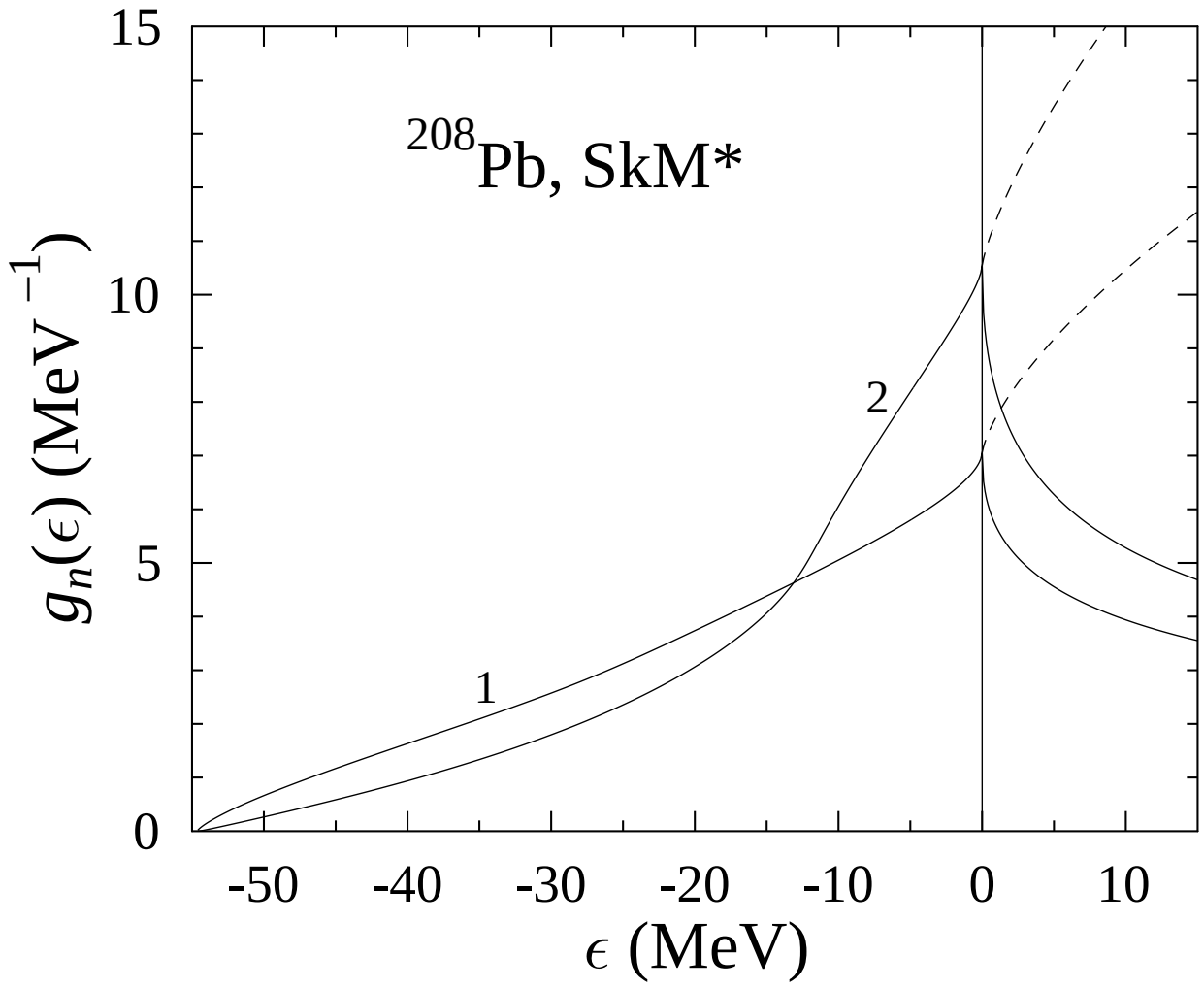

FIG. 5. The neutron single-particle level density $g_n(\epsilon)$ for the nucleus ^{208}Pb for the ETF +SkM* selfconsistent potential $V_n(r)$ with $m^*_{q,\omega}(r)/m = 1$ (curve 1) and the modified potential $V^*_q(r)$ from Eq. (34) use Eq. (33) (curve 2). The solid lines is obtained with subtracting of the free space states $g_{\rm free}(\epsilon)$ and the dashed lines are in presence of the spurious free-gas states.

In Fig. 6 we have plotted the number of states $N(\epsilon)$ embedded in ETF potential with energy below ϵ evaluated within the Thomas-Fermi approximation (solid line) in comparison with the $\hbar^2$-correction $N_{\rm corr}(\epsilon)$ from Eq. (34) (dashed line). As seen from Fig. 6, the $\hbar^2$-correction $N_{\rm corr}(\epsilon)$ is negligibly small, i.e., the corrections due to the ETF approximation play a minor role in the derivation as the Fermi energy ϵ_F well as the single-particle level density $g(\epsilon)$ (see also Ref. [21]).

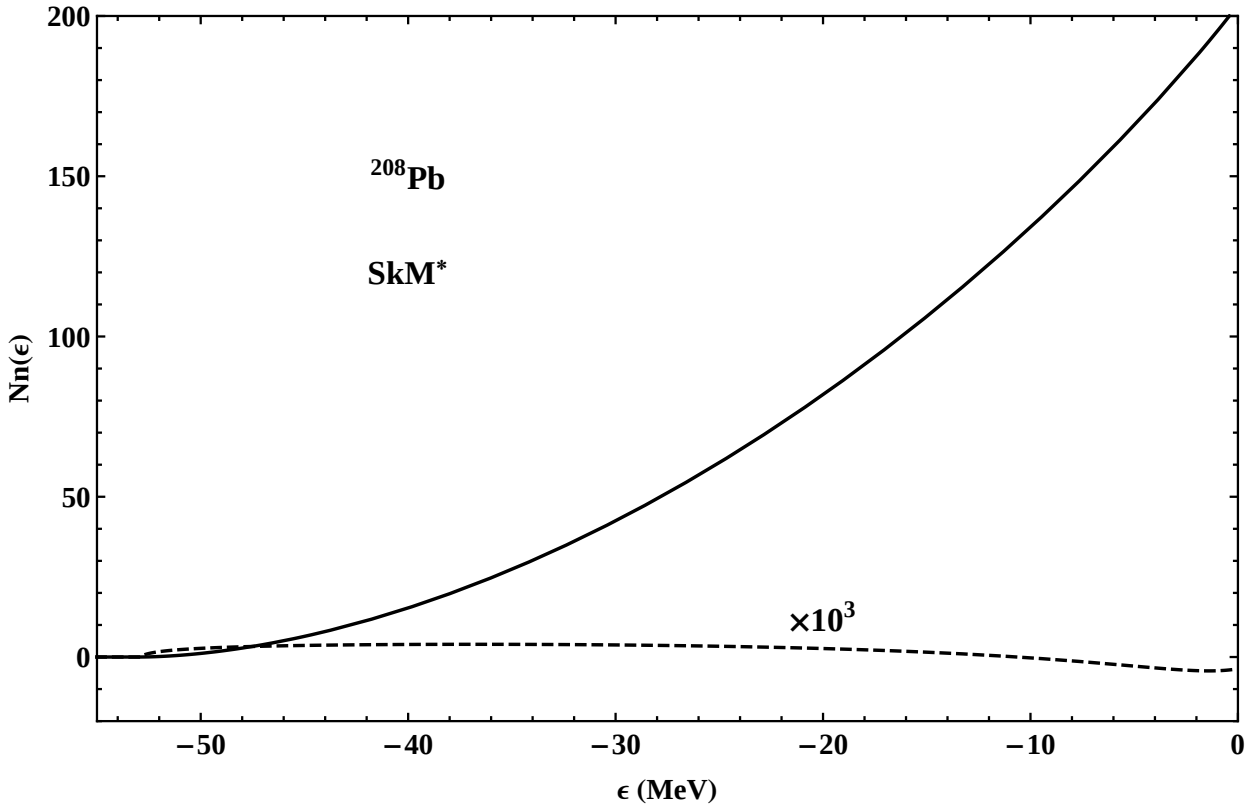

FIG. 6. The number of neutron states $N_n(\epsilon)$ within Thomas-Fermi approximation given by Eq. (27) (solid line) and the $\hbar^2$-correction $N_{n,\mathrm{corr}}(\epsilon)$ of Eq. (34) (dashed line) for the nucleus ^{208}Pb for Skyrme interaction SkM* [39].

IV. STATISTICAL INVERSE LEVEL DENSITY PARAMETER.

Assuming the Landau's conception of Fermi-gas of quasiparticles (see Fig. 1), we will apply Eq. (4) to evaluate the nuclear excitation energy E_{ex}. In the numerical calculations of the statistical level density parameters a_q we use Eq. (3) where the excitation energy E_{ex} for neutrons and protons are given by Eq. (4) with the Fermi's occupation numbers

$$n_q(\epsilon, T) = \frac{1}{1 + \exp\left[(\epsilon - \epsilon_{F,q}(T))/T\right]}.$$

The temperature dependent Fermi-energy $\epsilon_{F,q}(T)$ is obtained from the condition of the conservation of the particle number

$$N = \int_0^\infty d\epsilon\ \widetilde{g}^*_{\mathrm{TF},n}(\epsilon)\ n_n(\epsilon, T), \quad Z = \int_0^\infty d\epsilon\ \widetilde{g}^*_{\mathrm{TF},p}(\epsilon)\ n_p(\epsilon, T). \tag{35}$$

TABLE II. The results of calculations of the level density parameters a_q and K for different spherical nuclei. The calculations were performed within the ETF approximation by use Eqs. (7) and (32) for Skyrme interactions SkM* [39] and KDE0v1 [45]. In brackets, one shows the results with the effective ω-mass $m^*_{q,\omega}(r)/m = 1$.

	a_n, SkM*(MeV^{-1})	a_p, SkM*(MeV^{-1})	K, SkM*(MeV)	a_n,KDE0v1	a_p,KDE0v1	K,KDE0v1
^{40}Ca	2.47 (1.71)	2.51 (1.75)	8.03 (11.57)	2.35 (1.61)	2.38 (1.64)	8.45 (12.30)
^{48}Ca	3.31 (2.30)	2.63 (1.80)	8.09 (11.71)	3.08 (2.12)	2.52 (1.70)	8.58 (12.57)
^{90}Zr	5.70 (3.84)	4.98 (3.34)	8.43 (12.53)	5.32 (3.54)	4.76 (3.14)	8.94 (13.48)
^{120}Sn	7.80 (5.21)	6.28 (4.21)	8.52 (12.73)	7.22 (4.76)	6.03 (3.94)	9.06 (13.79)
^{208}Pb	13.67 (8.98)	10.42 (6.96)	8.64 (13.05)	12.57 (8.13)	10.07 (6.47)	9.19 (14.25)

Note that for calculations for the statistical level density parameters a_q in Table II and Fig. 7, we have used the low temperature $T \leq 2$ MeV to avoid the influence of the temperature dependence of the mean field $V_q(r)$ and the continuum effects on $g(\epsilon)$. In this case, the temperature dependence of Fermi energy is given by $\epsilon_F(T) = \epsilon_{F0} + \xi_2\ T^2 + \xi_4\ T^4 + O(T^6)$, see Appendix A. Here, the coefficients ξ_2 and ξ_4 are obtained from the condition of the conservation of the particle number (see Eqs. (A6) and (A7) in Appendix A).

Evaluating the statistical level density parameters a_q from Eqs. (3) and (4), we obtain also the statistical inverse level density parameter

$$K = \frac{A}{a_n + a_p}. \tag{36}$$

In Table II we show the results of calculations of the level density parameters a_q and K for the spherical nuclei ^{40}Ca, ^{48}Ca, ^{90}Zr, ^{120}Sn and ^{208}Pb. All results were obtained within the ETF approximation for Skyrme interactions SkM* and KDE0v1.

Fig. 7 shows a comparison of the experimental data (solid points) with the evaluated values of K within the ETF approximation from Table II. The experimental trend of the smooth inverse level-density parameter K can be be well reproduced by the following empirical relation, see Refs. [25, 30],

$$K(A) = K_0 + \kappa\,\frac{E_{\rm ex}}{A}\ , \quad K_0 = 7.8\ \text{MeV}, \quad \kappa = 0.00517\exp(0.0345A)\ . \tag{37}$$

The value of κ in Eq. (37) was obtained by a fit to the light particles evaporation spectra.

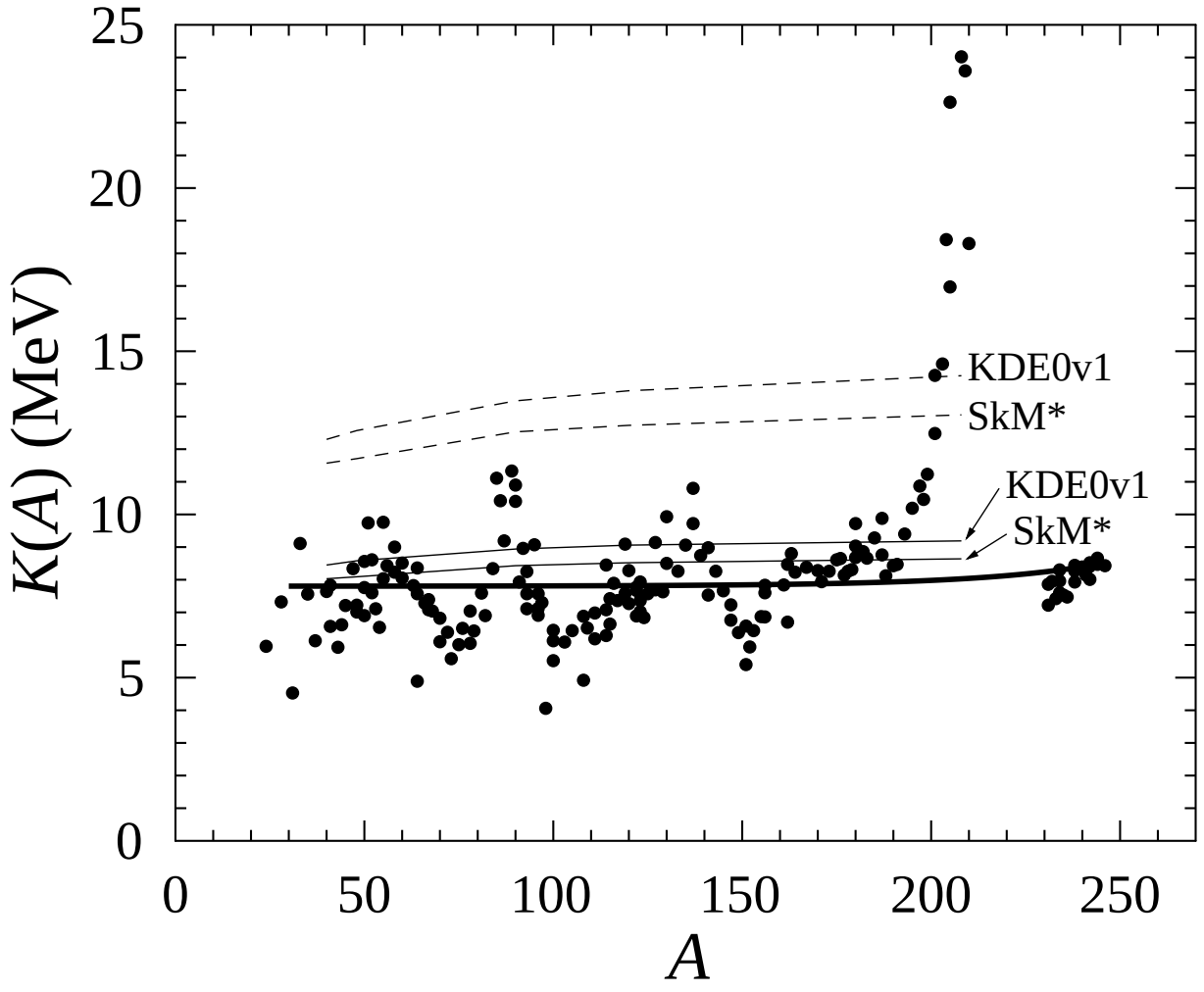

FIG. 7. Experimental values of K (solid points) from Ref. [5]. The thin solid lines represent the ETF calculations for Skyrme interactions SkM* and KDE0v1 (from Table 2) with effective mass $m^*_{q,\omega}(r)$ from Eq. (29). The dashed lines are for the case $m^*_{q,\omega}(r) = m$. The numerical calculations were performed by use of Eqs. (7) and (32). The thick solid line is the experimental fit from Eq. (37).

Thick solid line in Fig. 7 shows the value of K obtained by use of Eq. (37) for $E_{\rm ex} = 7$ MeV which is about of the neutron separation energy.

The results of Fig. 7 demonstrate a quite satisfactory description of average behavior of A-dependence of the statistical level-density parameter K obtained within the ETF approximation with Skyrme interaction. We point out two aspects which are important for the description: (i) the Landau's conception of quasiparticles near the Fermi surface which pro-

vides the use of simple gas model for the single particle level density $g(\epsilon)$, (ii) the accounting of the correlation corrections to the effective mass (frequency-dependent effective ω-mass $m^*_{q,\omega}(r)$) which enhances the level density $g(\epsilon)$ near the Fermi surface. A non-monotonic behavior of $K(A)$ in the experimental data in Fig. 7 is caused by the shell effects and can not be described within the semiclassical ETF approach used in this work.

V. CALORIC PROPERTIES OF HOT NUCLEI

The contribution of the continuum states to the single-particle level density $g(\epsilon)$ does not affect significantly the thermodynamic calculations, in particular, the statistical inverse level-density parameter K for low temperatures $T \lesssim 2$ MeV. However the procedure of correct subtracting of the free space states from $g(\epsilon)$ (see Section III) can play an appreciable role for higher temperatures. Considering a hot nucleus, the temperature dependences of the parameters in the particle density $\rho_q(\mathbf{r})$ in Eq. (23) as well as the effective mass $m^*_{q,\omega}(r)$ must be taken into account. All of them influence the effective mean field $V^*_q(r)$, see Eq. (29), and thereby the Fermi energy $\epsilon_{F,q}(T)$, the excitation energy $E_{\rm ex}(T)$, the entropy $S(T)$, etc. Note that the temperature dependence of the effective k-mass $m^*_{q,k}(r)$ occurs because of the mean field $V^*_q(r)$. We point out however that the involvement of the temperature dependence into the particle density $\rho_q(\mathbf{r},T)$ and the ω-mass $m^*_{q,\omega}(r)$ requires some caution. Both of them affect the mean field $V^*_q(r,T)$ and thereby the single-particle level density $g_q(\epsilon,T)$. This fact violates the fundamental relation of Eq. (4) for the excitation energy $E_{{\rm ex},q}(T)$ and can lead to a decrease of the entropy $S(T)$ with the increasing temperature T. To avoid this non-physical effect, the additional contribution from the temperature broadening of the heated nucleus has to be taken into account.

Performing the evaluation of the temperature dependence of the Fermi energy $\epsilon_{F,q}(T)$, we will apply the conditions of Eq. (35). Fig. 8 shows the difference in the dependence of the Fermi energy of neutrons $\epsilon_{F,n}(T)$ on the temperature in two cases if the continuum effects are ignored (dashed and dotted lines) and if these effects are taken into account (solid line).

The influence of the continuum corrections to the single-particle level density $g(\epsilon)$ on the nuclear caloric curve $E_{\rm ex}(T)$ and thereby on the statistical level parameter a is shown in

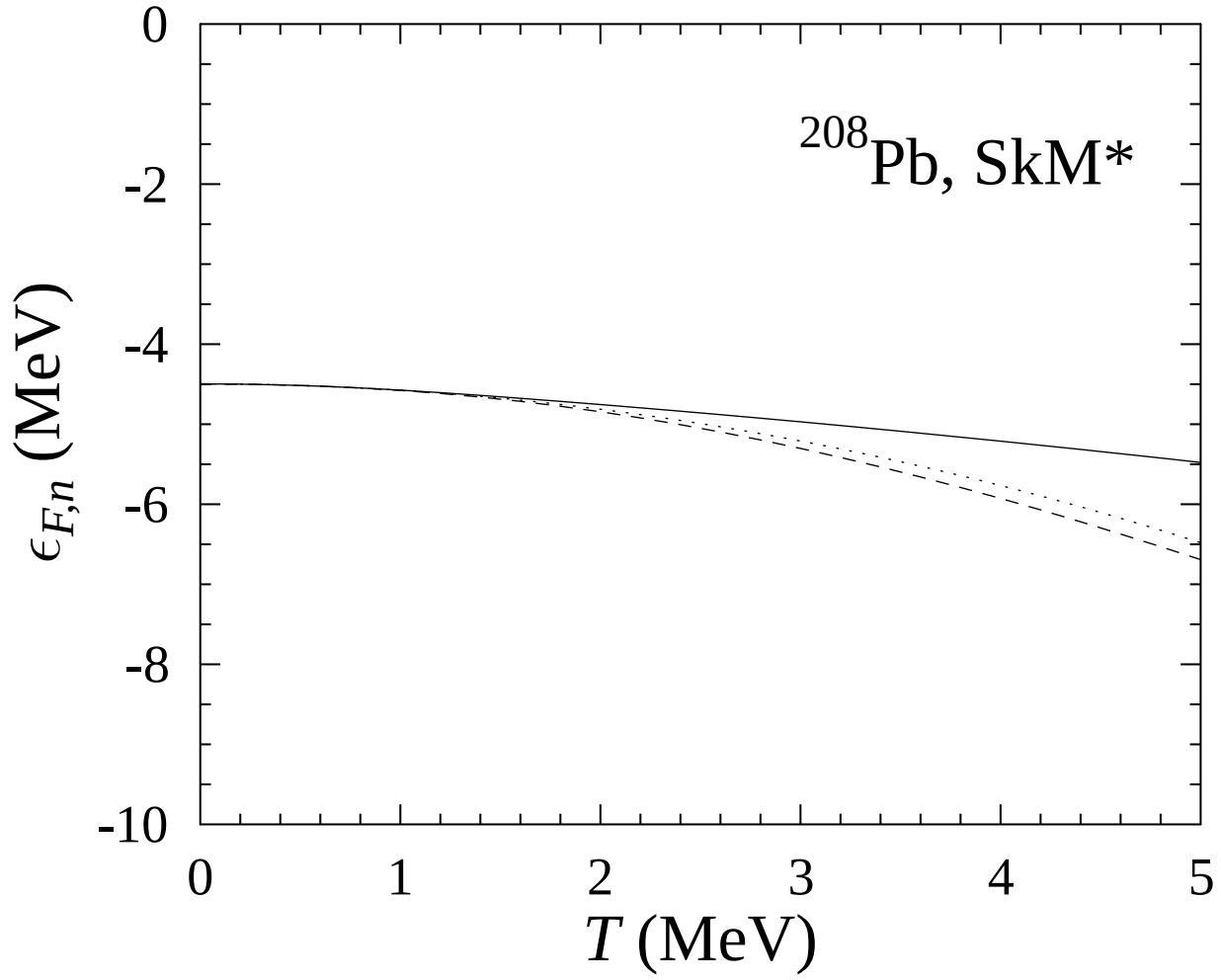

FIG. 8. The dependence of the separation energy of neutron $\epsilon_{F,n}(T)$ in the nucleus ^{208}Pb on the temperature. The solid line was obtained by use Eq. (35) taking into account the continuum effects. The dashed and dotted lines are for the case where such kind of effects are ignored: dashed line was obtained from Eq. (35) and dotted line is the commonly used result for $\epsilon_{F,n}(T)$ where the correction term up to $\sim T^2$ is only taken into account, see Eq. (A5) of Appendix A.

Fig. 9.

As seen from Fig. 9, the subtracting of the free-state contribution $g_{\rm free}(\epsilon)$ from the continuum states reduces significantly the result for the excitation energy $E_{n,\rm ex}$ in the case of high enough temperatures (compare solid and dashed lines). Note that the correct description of continuum states is especially important in the case of nuclei beyond the stability line where the Fermi energy is located close to the edge of potential well. A comparison of the dotted and dashed lines in Fig. 9 shows the influence of the high order terms in the T-expansion

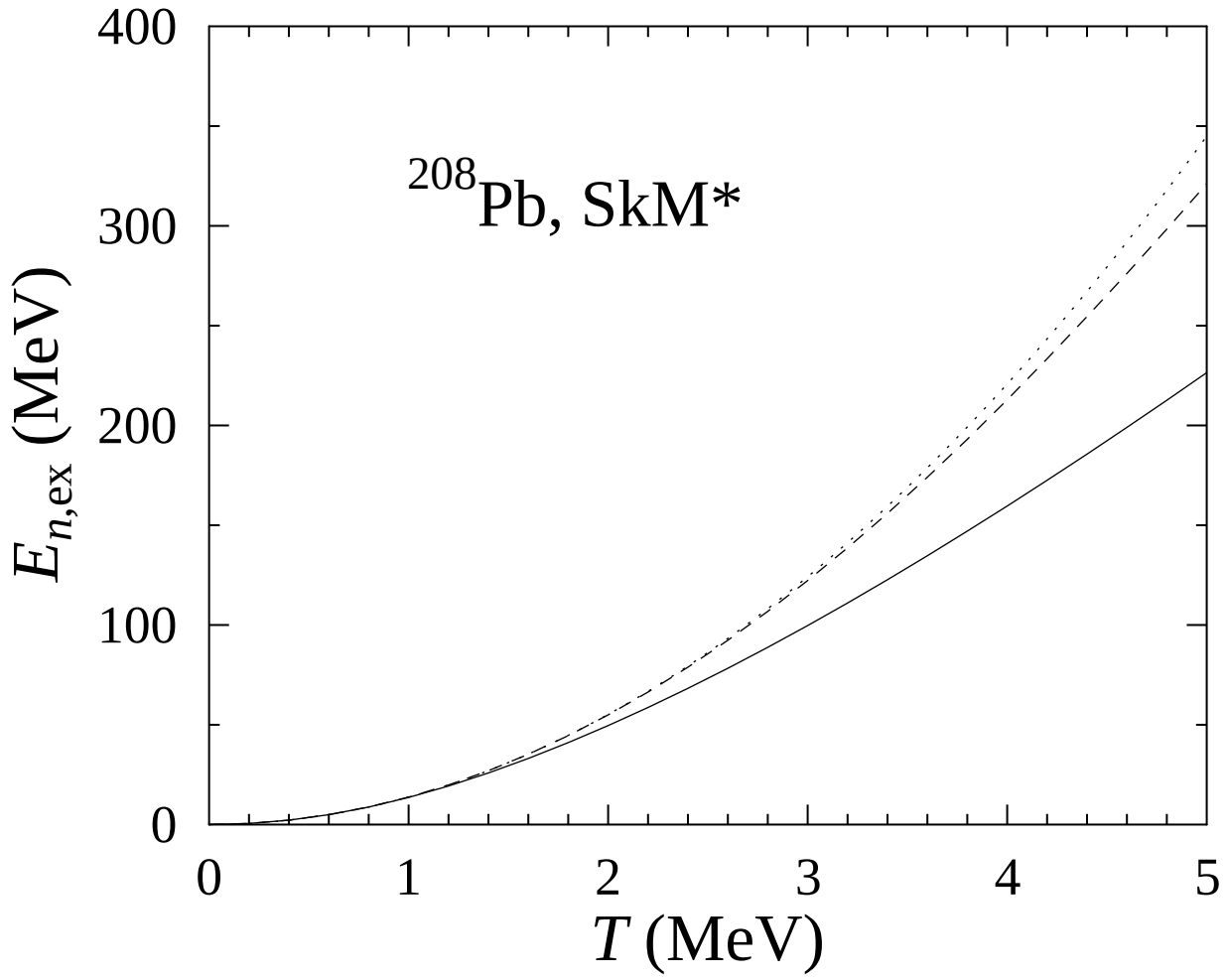

FIG. 9. The caloric curve $E_{\mathrm{ex}}(T)$ for the nucleus ^{208}Pb for the SkM* mean field. The dashed line is for the case without of subtracting of the free space contribution $N_{\mathrm{free}}(\epsilon)$ (see Eq. (25)) from the continuum, the solid line represents the result where the contribution of the continuum states were corrected according to Eqs. (7) and (32). The dotted line for a simple $E_{n,\mathrm{ex}}(T) = aT^2$ with constant a from Eq. (2).

of the caloric curve, see Eq. (A8) in Appendix A. In Fig. 9 we have taken into account the temperature dependence of the Fermi energy $\epsilon_{F,q}(T)$ (see Eq. (A5) in Appendix A) but ignored the temperature dependence of the mean field as well as the effective mass m_q^*.

Note that the caloric curve $E_{\mathrm{ex}}(T)$ (solid line in Fig. 9) behaves as $\sim T^2$ (degenerate Fermi-gas regime) at low temperatures and tends to the linear behavior $\sim T$ at higher temperatures, as it should be for the Boltzman gas regime. This fact provides the temperature dependence of the statistical level density parameters $a(T)$ and $K(T)$. The corresponding

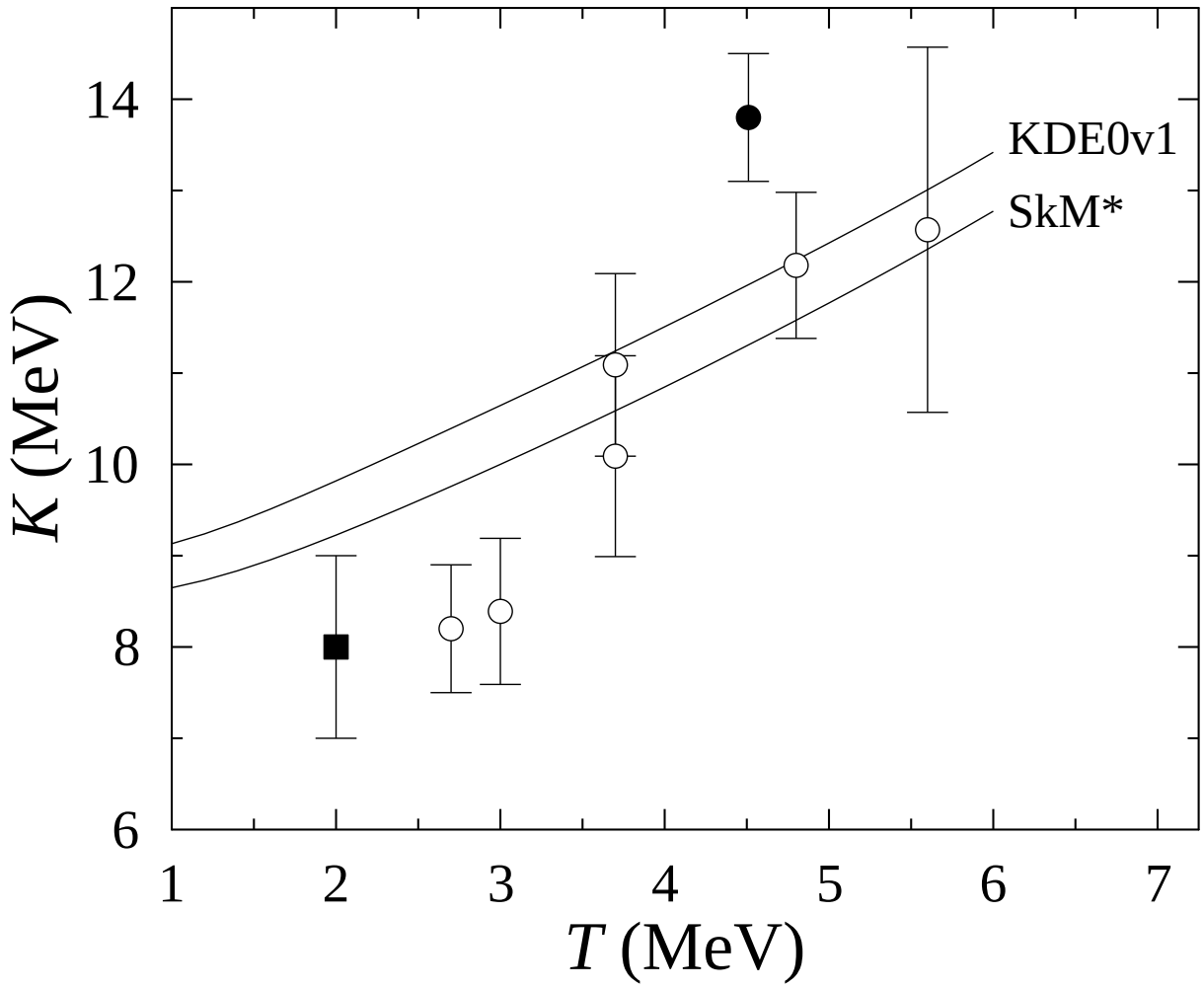

FIG. 10. The temperature dependence of the inverse statistical level-density parameter $K(T)$ for the nucleus with $Z = 64$ and $A = 160$ for Skyrme interactions SkM* and KDE0v1. The experimental data are taken from Refs. [12, 34, 35]

result for the statistical inverse level-density parameter $K(T)$ for the nucleus with $Z = 64$ and $A = 160$ is shown in Fig. 10.

A reasonable agreement with the experimental data in Fig. 10 is obtained by use of the selfconsistent mean field $V_q(r)$ with the nucleon density $\rho_q(\mathbf{r})$ given by Eq. (23) and Table I, and ignoring the temperature dependence in ω-mass $m^*_{q,\omega}(r)$.

VI. SUMMARY AND CONCLUSIONS

In the present work, we have applied the thermodynamical approach to a study of the statistical level density $\varrho(E_{\rm ex})$. The approach is based on the the extended Thomas-Fermi approximation (ETF) with Skyrme forces. The adopted approach describes successfully the basic nuclear liquid-drop properties as well as the single particle characteristics related to the nuclear mean field. The used ETF approximation with Skyrme forces can be considered as an unification of both fundamental nuclear models: the liquid drop model and the shell model. In a practical sense, this approach allows us to evaluate the quantum single-particle corrections to the bulk liquid drop characteristics, in particular, the shell corrections to the mass formula and the deformation energy. An advantage of this approach is that the nuclear mean field is consistent with the nuclear liquid drop because both of them are generated by the common Skyrme forces.

To evaluate the statistical level density $\varrho(E_{\rm ex})$ we need to know the excitation energy $E_{\rm ex}$ which is a complicate problem for a system of strongly interacting particles like a nucleus. We pointed out that a significant progress is achieved by use of the Landau's conception of quasiparticles where the excitation energy $E_{\rm ex}$ is derived within a Fermi-gas system of noninteracting quasiparticles and thereby depends on the mean field $V(\mathbf{r})$ and the effective mass m^* of the quasiparticle. In our consideration, the nuclear mean field $V(\mathbf{r})$ and the single-particle level density $g(\epsilon)$ are derived within the ETF with the effective SkM* and KDE0v1 Skyrme interactions. Using the Wigner distribution function in phase space $f(\mathbf{r},\mathbf{p})$, we have presented a semiclassical derivation of the single-particle level density $g(\epsilon)$ and the number of states $N(\epsilon)$ embedded in potential well $V(\mathbf{r})$ with energy below ϵ. Analyzing the value of $N(\epsilon)$, we have shown that the $\hbar^2$-corrections to $N(\epsilon)$ play only a minor role.

Applying the Landau's conception of quasiparticles, we have evaluated the excitation energy $E_{\rm ex}$ and the statistical inverse level density parameter K of the nucleus. As it can be seen from Fig. 1, the evaluation of the excitation energy $E_{\rm ex}$ needs the single particle states near Fermi energy only. This fact confirms the Landau's conception of quasiparticles and allows one to use the Fermi-gas expression (4) to evaluate the nuclear excitation energy. Involving the effective mass $m^*(r)$ of quasiparticles, we took into consideration both contributions to $m^*(r)$ caused by the non-locality of the nucleon-nucleus interaction (k-mass $m^*_k(r)$) which is generated by the Skyrme interaction and the correlation correc-

tion (frequency dependent ω-mass $m^*_\omega(r)$) which arises from the scattering of nucleons from low-lying surface vibrations of the nucleus [50]. We show (see Fig. 4) that the presence of the frequency dependent ω-mass $m^*_\omega(r)$ distorts significantly the selfconsistent mean field and leads to the enhancement of the single particle level density near the Fermi surface (see Fig. 5). We have shown (see Fig. 7) that the ETF approximation with Skyrme interaction provides a quite satisfactory description of average A-dependence of the statistical inverse level density parameter K.

Using the ETF finite-depth potential $V(\mathbf{r})$, we have paid a special attention to the accuracy of the derivation of the level density $g(\epsilon)$ in continuum at $\epsilon > 0$. The subtraction of the free space contribution from $g(\epsilon)$ allows one to prevent a spurious contribution to the excitation energy $E_{\rm ex}$. A spurious contribution to $E_{\rm ex}$ occurs due to the free space states which are not associated with the potential well $V(\mathbf{r})$. Our numerical calculations for the Skyrme ETF potential show that the correct subtraction of the free-state contribution from the continuum states reduces strongly the result for the excitation energy $E_{\rm ex}$ and thereby increases the result for K in the case of high enough temperatures, see Figs. 9 and 10.

VII. ACKNOWLEDGEMENTS

This work was supported in part by the National Academy of Sciences of Ukraine under grant # CO-2-14/2016 (V. M. K.) and by the US Department of Energy under contract # DOE-FG03-93ER40773 (S. S.). S. Shlomo also thanks the Weizmann Institute for the Weston Visiting Professorship Award and the nice hospitality extended to him.

APPENDIX A. EXCITATION ENERGY OF A FERMI GAS

In a simplest Fermi gas model assuming that the mean field $V(r)$ is temperature independent, the total energy $E(T)$ is given by the following expression, see Ref. [40], Sect. #58,

$$E(T) = \int_0^\infty d\epsilon\ \epsilon\ g(\epsilon)\ n(\epsilon,T) = \int_0^{\epsilon_F(T)} d\epsilon\ \epsilon\ g(\epsilon) + \frac{\pi^2}{6}\ \frac{d\epsilon g(\epsilon)}{d\epsilon}\bigg|_{\epsilon=\epsilon_F(T)} T^2 \qquad \text{(A1)}$$
$$+\frac{7\pi^4}{360}\ \frac{d^3\epsilon g(\epsilon)}{d\epsilon^3}\bigg|_{\epsilon=\epsilon_F(T)} T^4 + O(T^6),$$

where $g(\epsilon)$ is the single particle level density of the Fermi gas and the occupation numbers $n(\epsilon, T)$ are given by the Fermi function

$$n(\epsilon, T) = \frac{1}{1 + \exp\left[(\epsilon - \epsilon_F(T))/T\right]}. \tag{A2}$$

The Fermi energy $\epsilon_F(T)$ in Eq. (A2) is temperature dependent. The temperature dependence of $\epsilon_F(T)$ is obtained from the condition of conservation of the particle number A :

$$A = \int_0^\infty d\epsilon \;\; g(\epsilon)\; n(\epsilon, T). \tag{A3}$$

Similarly to Eq. (A1) one can rewrite Eq. (A3) as a T-expansion

$$A = \int_0^{\epsilon_F(T)} d\epsilon\; g(\epsilon) + \frac{\pi^2}{6} g'[\epsilon_F(T)]\; T^2 + + \frac{7\pi^4}{360} g'''[\epsilon_F(T)]\; T^4 + O(T^6). \tag{A4}$$

Keeping the terms up to T^4, we obtain from Eq. (A4)

$$\epsilon_F(T) = \epsilon_{F0} + \xi_2\; T^2 + \xi_4\; T^4 + O(T^6), \tag{A5}$$

where $\epsilon_{F0} = \epsilon_F(T = 0)$ and (to simplify notations we will use $g_F = g(\epsilon_{F0})$, $g'_F = g'(\epsilon_{F0})$, etc.)

$$\xi_2 = -\frac{\pi^2}{6} \frac{g'_F}{g_F}, \tag{A6}$$

$$\xi_4 = -\frac{1}{g_F} \left[\frac{1}{2}\; g'_F\; \xi_2^2 + \frac{\pi^2}{6}\; g''_F\; \xi_2 + \frac{7\pi^4}{360} g'''_F \right]. \tag{A7}$$

Note that the expansion of Eq. (A1) implies that the density $g(\epsilon)$ is a sufficiently smooth function of ϵ. The subtraction of continuum states from $g(\epsilon)$ leads to a cusp at $\epsilon = 0$ (see Fig. 4) and the expansion of Eq. (A1) can not be applied. In this case, the numerical solution of Eq. (A3) with respect to $\epsilon_F(T)$ must be used.

Let us rewrite Eq. (A1) as

$$E(T) = \int_0^{\epsilon_F(T)} d\epsilon\; \epsilon\; g(\epsilon) + \frac{\pi^2}{6} [g(\epsilon_F(T)) + \epsilon_F(T)\; g'(\epsilon_F(T))]\; T^2$$
$$+ \frac{7\pi^4}{360} [3\; g''(\epsilon_F(T)) + \epsilon_F(T)\; g'''(\epsilon_F(T))]\; T^4 + O(T^6). \tag{A8}$$

Using the definition of the ground state energy E_0 of a Fermi gas

$$E_0 = \int_0^{\epsilon_{F,0}} d\epsilon \ \epsilon \ g(\epsilon)$$

and Eqs. (A6) and (A7), one obtains the excitation energy $E_{\rm ex}$ in the following form

$$\begin{aligned} E_{\rm ex} &= E(T) - E_0 \\ &= \frac{\pi^2}{6} \ g_F \ T^2 + g_F \left[\frac{7\pi^4}{120} \frac{g_F''}{g_F} - \frac{\pi^4}{24} \left(\frac{g_F'}{g_F} \right)^2 \right] \ T^4 + O(T^6). \end{aligned} \tag{A9}$$

One can see from Eq. (A9) that the derivatives of the single particle level density $g(\epsilon)$ influence on the excitation energy in the higher order of the temperature $\sim T^4$ only. Note also that the expression (A9) was obtained by use of the expansion (A5) for the Fermi energy $\epsilon_F(T)$ and can not be used at high temperatures where the continuum states in $g(\epsilon)$ play an appreciable role.

APPENDIX B. ETF MEAN FIELD $V_q(\mathbf{r})$ WITH SKYRME INTERACTION

We will consider the nucleon mean field $V_q(\mathbf{r})$ derived by Eq. (24). Using the potential energy $E_{\rm pot}$ for Skyrme interaction [39, 41] one obtains the mean field $V_q(\mathbf{r})$ in the following form

$$V_q = V_q^\rho + V_q^J. \tag{B1}$$

Here V_q^ρ is given by

$$\begin{aligned} V_q^\rho = & \ t_0 \left(1 + \frac{1}{2} x_0 \right) \ \rho - t_0 \left(x_0 + \frac{1}{2} \right) \ \rho_q \\ & + \frac{\alpha+2}{12} t_3 \ \left(x_3 + \frac{1}{2} \right) \ \rho^{\alpha+1} - \frac{\alpha}{12} t_3 \ \left(\frac{1}{2} + x_3 \right) \rho^{\alpha-1} \left[\rho_n^2 + \rho_p^2 \right] \\ & - \frac{1}{6} t_3 \ \left(x_3 + \frac{1}{2} \right) \ \rho_q^\alpha \rho_q - \frac{1}{8} \left[3 \ t_1 \left(1 + \frac{1}{2} x_1 \right) - t_2 \ \left(1 + \frac{1}{2} x_2 \right) \right] \ \nabla^2 \rho \\ & + \frac{1}{8} \left[3 \ t_1 \left(\frac{1}{2} + x_1 \right) + t_2 \ \left(\frac{1}{2} + x_2 \right) \right] \ \nabla^2 \rho_q \\ & + \frac{1}{4} \left[t_1 \left(1 + \frac{1}{2} x_1 \right) + t_2 \ \left(1 + \frac{1}{2} x_2 \right) \right] \tau_{\rm kin} - \frac{1}{4} \left[t_1 \left(x_1 + \frac{1}{2} \right) - t_2 \ \left(x_2 + \frac{1}{2} \right) \right] \tau_{q,\rm kin} \\ & - \frac{1}{2} W_0 \ (\nabla \cdot \mathbf{J} + \nabla \cdot \mathbf{J}_q) + \delta_{qp} \ e^2 \left[\int d\mathbf{r}' \frac{1}{|\mathbf{r} - \mathbf{r}'|} - \left(\frac{3}{\pi} \rho_p \right)^{1/3} \right]. \end{aligned} \tag{B2}$$

Here, the factor $\tau_{q,\mathrm{kin}}$ is related to the kinetic energy density $\epsilon_{q,\mathrm{kin}} = (\hbar^2/2m)\tau_{q,\mathrm{kin}}$. In the case of the ETF approximation, the factor $\tau_{q,\mathrm{kin}}$ is given by [39, 43]

$$\begin{aligned}\tau_{q,\mathrm{kin}} = & \frac{3}{5}(3\pi^2)^{2/3}\rho_q^{5/3} + \frac{1}{36}\frac{(\nabla\rho_q)^2}{\rho_q} + \frac{1}{3}\nabla^2\rho_q \\ & + \frac{1}{6}\frac{\nabla\rho_q\cdot\nabla f_q}{f_q} + \frac{1}{6}\rho_q\frac{\nabla^2 f_q}{f_q} - \frac{1}{12}\rho_q\frac{(\nabla f_q)^2}{{f_q}^2} \\ & + \frac{1}{2}\left(\frac{2m}{\hbar^2}\right)^2\rho_q\left(\frac{\mathbf{W}_q}{f_q}\right)^2 \end{aligned} \tag{B3}$$

where f_q is related to the nucleon effective mass $m^*_{q,k}$ as

$$\begin{aligned} f_q \equiv \frac{m}{m^*_{q,k}} = & 1 + \frac{2m}{\hbar^2} \\ & \times\left(\frac{1}{4}\left[t_1\left(1+\frac{1}{2}x_1\right) + t_2\left(1+\frac{1}{2}x_2\right)\right]\rho - \frac{1}{4}\left[t_1\left(x_1+\frac{1}{2}\right) - t_2\left(x_2+\frac{1}{2}\right)\right]\rho_q\right) \end{aligned} \tag{B4}$$

and $\mathbf{W}_q$ is related to the spin-orbit interaction

$$\mathbf{W}_q = \frac{1}{2}W_0(\nabla\rho + \nabla\rho_q) \tag{B5}$$

with the spin-orbit constant W_0. In Eq. (B2), the spin-orbit current density $\mathbf{J}_q$ is derived as

$$\mathbf{J}_q = \frac{2m}{\hbar^2}\frac{\rho_q}{f_q}\mathbf{W}_q. \tag{B6}$$

We use also the notations

$$\rho = \rho_n + \rho_p, \quad \tau_{\mathrm{kin}} = \tau_{n,\mathrm{kin}} + \tau_{p,\mathrm{kin}}, \quad \mathbf{J} = \mathbf{J}_n + \mathbf{J}_p.$$

Finally, the mean field V_q^J in Eq. (B1) is given by

$$V_q^J = -\frac{2m}{\hbar^2}(\mathbf{W}_q)^2 D_{q,1} - \frac{2m}{\hbar^2}(\mathbf{W}_{\widetilde{q}})^2 D_{\widetilde{q},2} - \frac{1}{2}W_0\ \left(\nabla\cdot\mathbf{J} + \nabla\cdot\mathbf{J}_q\right), \tag{B7}$$

where

$$D_{q,1} = \frac{1}{f_q} - \frac{2m}{\hbar^2}\left[\frac{1}{8}t_1(1-x_1) + \frac{3}{8}t_2(1+x_2)\right]\frac{\rho_q}{{f_q}^2}, \tag{B8}$$

$$D_{\widetilde{q},2} = -\frac{2m}{\hbar^2}\left[\frac{1}{4}t_1\left(1+\frac{1}{2}x_1\right) + \frac{1}{4}t_2\left(1+\frac{1}{2}x_2\right)\right]\frac{\rho_{\widetilde{q}}}{{f_{\widetilde{q}}}^2}. \tag{B9}$$

In Eqs. (B7), (B8) and (B9), we have used the notations $\widetilde{q} = p$ if $q = n$ and *vice versa*.

APPENDIX C. ENERGY-DEPENDENT PARTICLE DENSITY $\rho_\epsilon(\mathbf{r})$

Considering particle density $\rho_\epsilon(\mathbf{r})$, we will apply the direct variational method [36] and assume the following form for each sort of nucleons, see Eq. (23),

$$\rho_\epsilon(\mathbf{r}) = \rho_{0,\epsilon}\left[1+\exp\left(\frac{r-R}{d}\right)\right]^{-\eta}, \tag{C1}$$

where the profile parameters R, d and η are the same as the ones in the $\rho_{\rm eq}(\mathbf{r})$, see Eq. (23) and Table I. In the case of the TF approximation, the value of $\rho_{0,\epsilon}$ is normalized by the condition (11) which provides

$$\rho_{0,\epsilon} = \frac{N_{\rm TF}(\epsilon)}{D_0}, \tag{C2}$$

where

$$D_0 = \int d\mathbf{r}\ \left[1+\exp\left(\frac{r-R}{d}\right)\right]^{-\eta}.$$

In the case of ETF approximation, the particle density $\rho_\epsilon(\mathbf{r})$ is normalized by the condition

$$N_{\rm ETF}(\epsilon) = \int d\mathbf{r}\ \rho_\epsilon(\mathbf{r}). \tag{C3}$$

Using Eq. (18) and Eq. (C3), we obtain

$$N_{\rm ETF}(\epsilon) = N_{\rm TF}(\epsilon) - \frac{1}{48\ \pi^2}\frac{2m}{\hbar^2}\frac{1}{(3\pi^2)^{1/3}}[N_{\rm TF}(\epsilon)/D_0]^{-1/3}D_1, \tag{C4}$$

where

$$D_1 = \int d\mathbf{r}\ \left[1+\exp\left(\frac{r-R}{d}\right)\right]^{\eta/3}\nabla^2 V(\mathbf{r}).$$

Solving Eq. (C4) with respect to $N_{\rm ETF}(\epsilon)$, one can find the correction $\Delta N(\epsilon) = N_{\rm ETF}(\epsilon) - N_{\rm TF}(\epsilon)$ to the number of state $N(\epsilon)$ and thereby to the single-particle level density $g(\epsilon)$ caused by the gradient terms in the semiclassical approximation. In the first order, one obtains from Eq. (C4)

$$\Delta N(\epsilon) = -\frac{1}{48\ \pi^2}\frac{2m}{\hbar^2}\frac{1}{(3\pi^2)^{1/3}}[N_{\rm TF}(\epsilon)/D_0]^{-1/3}D_1, \tag{C5}$$

---

[1] T. Ericson, Adv. in Phys. **9**, 425 (1960).

[2] A. Bohr and B.R. Mottelson, *Nuclear Structure*, Vol. I (W.A. Benjamin, New York, 1969).

[3] A. Gilbert and A. Cameron, Can. J. Phys. **43**, 1446 (1965).

[4] J.R. Huizenga and L.G. Moretto, Ann. Rev. Nucl. Sci. **22**, 427 (1972).

[5] V.S. Stavinskii, Phys. of Part. and Nucl. **3**, 832 (1972).

[6] S.K. Kataria, V. S. Ramamurthy and S.S. Kapoor, Phys. Rev. C **18**, 549 (1978).

[7] A.V. Ignatyuk, Phys. Lett. **B76**, 543 (1979); Nucl. Phys. **A346**, 191 (1980).

[8] S. Shlomo and V.M. Kolomietz, Rep. Prog. Phys. **68**, 1 (2005).

[9] E.M. Lifshitz and L.P. Pitaevsky, *Statistical Physics: Theory of the Condensed State*, (Pergamon Press, Oxford - New York - Seoul - Tokyo, 1980).

[10] A.B. Migdal, *Theory of finite Fermi systems and properties of atomic nuclei* (Nauka, Moscow, 1983).

[11] D.R. Dean and U. Mosel, Z. Phys. **A322**, 647 (1985).

[12] S. Shlomo and J. B. Natowitz, Phys. Lett. **B252**, 187 (1990); Phys. Rev. C **44**, 2878 (1991).

[13] M. Prakash, J. Wambach and Z.Y. Ma, Phys. Lett. **B128**, 141 (1983).

[14] R. Hasse and P. Schuck, Phys. Lett. **B179**, 313 (1986).

[15] P.F. Bortignon and C. H. Dasso, Phys. Lett. **B189**, 381 (1987).

[16] J. Tõke and W.J. Swiatecki, Nucl. Phys. **A372**, 141 (1981).

[17] F. Garcias, M. Baranco, J. Nemeth and C. Ngo, Phys. Lett. **B206**, 177 (1988); M. Baranco and J. Treiner, Nucl. Phys. **A351**, 269 (1981).

[18] S. Bjørnholm, A. Bohr and B.R. Mottelson, in *Physics and chemistry of fission*, Vienna, IAEA 1974, p. 367.

[19] Y. Alhassid and B. Bush, Nucl. Phys. **A549**, 43 (1992); Nucl. Phys. **A565**, 399 (1993).

[20] B.K. Agrawal, S.K. Samaddar, J. N. De, and S. Shlomo, Phys. Rev. C **58**, 3004 (1998).

[21] S. Shlomo, Nucl. Phys. **A539**, 17 (1992).

[22] J.N. De, S. Shlomo and S.K. Samaddar, Phys. Rev. C **57**, 1398 (1998).

[23] N. Cerf, Phys. Rev. C **50**, 836 (1994).

[24] T. Rauscher, F-K. Thielemann and K-L. Kratz, Phys. Rev. C **56**, 1613 (1997).

[25] Pratap Roy, K. Banerjee, C. Bhattacharya, *et al.*, Phys. Rev. C **94**, 064607 (2016).

[26] P. Demetriou and S. Goriely, Nucl. Phys. **A 695**, 95 (2001).

[27] F. Minato, Nucl. Sci. Tech. **48**, 984 (2011).

[28] S. Bassauer, P. von Neumann-Cosel and A. Tamii, Phys. Rev. C **94**, 054313 (2016).

[29] R. Pezer, A. Venturab and D. Vretenar, Nucl. Phys. **A 717**, 21 (2003).

[30] R. J. Charity, Phys. Rev. C **82**, 014610 (2010).

[31] Ye.A. Bogila, V.M. Kolomietz, and A.I. Sanzhur, Z. Phys. **A 341**, 373 (1992).

[32] S. Shlomo, Ye.A. Bogila, V.M. Kolomietz and A.I. Sanzhur, Z. Phys. A **353**, 27 (1995).

[33] G. Nebbia, K. Hagel, D. Fabris *et al.*, Phys. Lett. B **176**, 20 (1986).

[34] K. Hagel, D. Fabris, P. Gonthier *et al.*, Nucl. Phys. **A 486**, 429 (1988).

[35] M. Gonin, L. Cooke, K. Hagel *et al.*, Phys. Rev. C **42**, 2125 (1990).

[36] V.M. Kolomietz and A.I. Sanzhur, Eur. Phys. J. A **38**, 345 (2008).

[37] V.M. Kolomietz, A.I. Sanzhur and B.V. Reznychenko, Inter. Journ. of Mod. Phys. E **25**, 2116 3, 1650016 (2016).

[38] V.M. Kolomietz, S.V. Lukyanov and A.I. Sanzhur, Phys. Rev. C **85**, 034309 (2012).

[39] M. Brack, C. Guet, and. H.-B. Håkansson, Phys. Rep. **123**, 275 (1985).

[40] L.D. Landau and E.M. Lifshitz, *Statistical Physics* (Pergamon Press, Oxford, 1958).

[41] P. Ring and P. Schuck, *The Nuclear Many-Body Problem* (Springer-Verlag, New-York, 1980).

[42] D.A. Kirzhnitz, *Field Theoretical Methods in Many Body Systems* (Pergamon, London, 1967).

[43] B. Grammaticos and A. Voros, Ann. of Phys. **123**, 359 (1979).

[44] G.A. Korn, and T.M. Korn, *Mathematical Handbook for Scientists and Engineers* (McGraw-Hill Book Company, New York/San Francisco/Toronto/London/Sydney 1968)

[45] B.K. Agrawal, S. Shlomo, and V.K. Au, Phys. Rev. C **72**, 014310 (2005).

[46] S. Shlomo, V.M. Kolomietz and H. Dejbakhsh, Phys. Rev. C **55**, 1972 (1997).

[47] D.L. Tubbes and S.E. Koonin, Astrophys. J. **232**, L59 (1979).

[48] C.A. Levinson, Danske Mat-fys. Medd. **25,** no. 9 (1949).

[49] F.G. Perey and B. Buck, Nucl. Phys. **32**, 353 (1962).

[50] G.E. Brown, J.H. Gunn and P. Gould, Nucl. Phys. **46**, 598 (1963).